

# ANALYSIS & PDE

Volume 11      No. 8      2018

ALLAN GREENLEAF, MATTI LASSAS, MATTEO SANTACESARIA,  
SAMULI SILTANEN AND GUNTHER UHLMANN

**PROPAGATION AND RECOVERY OF SINGULARITIES  
IN THE INVERSE CONDUCTIVITY PROBLEM**



## PROPAGATION AND RECOVERY OF SINGULARITIES IN THE INVERSE CONDUCTIVITY PROBLEM

ALLAN GREENLEAF, MATTI LASSAS, MATTEO SANTACESARIA,  
SAMULI SILTANEN AND GUNTHER UHLMANN

The ill-posedness of Calderón’s inverse conductivity problem, responsible for the poor spatial resolution of electrical impedance tomography (EIT), has been an impetus for the development of hybrid imaging techniques, which compensate for this lack of resolution by coupling with a second type of physical wave, typically modeled by a hyperbolic PDE. We show in two dimensions how, using EIT data alone, to use propagation of singularities for complex principal-type PDEs to efficiently detect interior jumps and other singularities of the conductivity. Analysis of variants of the CGO solutions of Astala and Päivärinta (*Ann. Math.* (2) **163**:1 (2006), 265–299) allows us to exploit a complex principal-type geometry underlying the problem and show that the leading term in a Born series is an invertible nonlinear generalized Radon transform of the conductivity. The wave front set of all higher-order terms can be characterized, and, under a prior, some refined descriptions are possible. We present numerics to show that this approach is effective for detecting inclusions within inclusions.

1. Introduction	1901
2. Complex principal-type structure of CGO solutions	1909
3. Conductivity equations and CGO solutions	1910
4. Fréchet differentiability and the Neumann series	1912
5. Fourier transform and the virtual variable	1916
6. Analysis of $\hat{\omega}_2$	1922
7. Higher-order terms	1927
8. Parity symmetry	1930
9. Multilinear operator theory	1931
10. Computational studies	1933
11. Conclusion	1938
References	1939

### 1. Introduction

Electrical impedance tomography (EIT) aims to reconstruct the electric conductivity,  $\sigma$ , inside a body from active current and voltage measurements at the boundary. In many important applications of EIT, such as medical imaging [Assenheimer et al. 2001; Cheney et al. 1999; Isaacson et al. 2006] and geophysical

---

Greenleaf is partially supported by DMS-1362271 and a Simons Foundation Fellowship, Lassas and Siltanen are partially supported by Academy of Finland, Uhlmann is partially supported by a FiDiPro professorship.

*MSC2010*: 35R30, 58J40, 65N21.

*Keywords*: electrical impedance tomography, propagation of singularities, Calderón’s problem, tomography, Radon transform.

prospecting, the primary interest is in detecting the location of interfaces between regions of inhomogeneous but relatively smooth conductivity. For example, the conductivity of bone is much lower than that of either skin or brain tissue, so there are jumps in conductivity of opposite signs as one transverses the skull.

In this paper we present a new approach in two dimensions to determining the singularities of a conductivity from EIT data. Analyzing the complex geometrical optics (CGO) solutions, originally introduced by Sylvester and Uhlmann [1987] and in the form required here by Astala and Päivärinta [2006a] and Huhtanen and Perämäki [2012], we transform the boundary values of the CGO solutions, which are determined by the Dirichlet-to-Neumann map [Astala and Päivärinta 2006b], in such a way as to extract the leading singularities of the conductivity,  $\sigma$ .

We show that the leading term of a Born series derived from the boundary data is a nonlinear Radon transform of  $\sigma$  and allows for good reconstruction of the singularities of  $\sigma$ , with the higher-order terms representing multiple scattering. Although one cannot escape the exponential ill-posedness inherent in EIT, the well-posedness of Radon inversion results in a robust method for detecting the leading singularities of  $\sigma$ . In particular, one is able to detect inclusions within inclusions (i.e., nested inclusions) within an unknown inhomogeneous background conductivity; this has been a challenge for other EIT methods. This property is crucial for one of the main applications motivating this study, namely using EIT for classifying strokes as ischemic (caused by an embolism preventing blood flow to part of the brain) or hemorrhagic (caused by bleeding in the brain); see [Holder 1992a; 1992b; Malone et al. 2014].

Our algorithm consists of two steps, the first of which is the reconstruction of the boundary values of the CGO solutions, and this is known to be exponentially ill-posed, i.e., satisfy only logarithmic stability estimates [Knudsen et al. 2009]. The second step begins with a separation of variables and partial Fourier transform in the radial component of the spectral variable. Thus, one instability of our algorithm arises from the exponential instability of the reconstruction of the CGO solutions from the Dirichlet-to-Neumann map. Another instability arises from low-pass filtering in Fourier inversion (similar to those of regularization methods used for CT and other linear inverse problems), and (presumably) the multiple scattering terms in the Born series we work with, which we only control rigorously for low orders and under some prior. Nevertheless, based on both the microlocal analysis and numerical simulations we present, the method appears to allow for robust detection of singularities of  $\sigma$ , in particular the location and signs of jumps. See Section 1A for further discussion of the ill-posedness issues raised by this method.

EIT can be modeled mathematically using the inverse conductivity problem of [Calderón 1980]. Consider a bounded, simply connected domain  $\Omega \subset \mathbb{R}^n$  with smooth boundary and a scalar conductivity coefficient  $\sigma \in L^\infty(\Omega)$  satisfying  $\sigma(x) \geq c > 0$  almost everywhere. Applying a voltage distribution  $f$  at the boundary leads to the elliptic boundary-value problem

$$\nabla \cdot \sigma \nabla u = 0 \quad \text{in } \Omega, \quad u|_{\partial\Omega} = f. \quad (1-1)$$

Infinite-precision boundary measurements are then modeled by the Dirichlet-to-Neumann map

$$\Lambda_\sigma : f \mapsto \sigma \frac{\partial u}{\partial \vec{n}} \Big|_{\partial\Omega}, \quad (1-2)$$

where  $\vec{n}$  is the outward normal vector of  $\partial\Omega$ .

Astala and Päivärinta [2006b] transformed the construction of the CGO solutions in two dimensions by reducing the conductivity equation to a Beltrami equation. Identify  $\mathbb{R}^2$  with  $\mathbb{C}$  by setting  $z = x_1 + ix_2$  and define the Beltrami coefficient

$$\mu(z) = \frac{1 - \sigma(z)}{1 + \sigma(z)}.$$

Since  $c_1 \leq \sigma(z) \leq c_2$ , we have  $|\mu(z)| \leq 1 - \epsilon$  for some  $\epsilon > 0$ . Further, if we assume  $\sigma \equiv 1$  outside some  $\Omega_0 \Subset \Omega$ , then  $\text{supp}(\mu) \subset \overline{\Omega}_0$ . Now consider the unique solution of

$$\bar{\partial}_z f_{\pm}(z, k) = \pm \mu(z) \overline{\partial_z f_{\pm}(z, k)}, \quad e^{-ikz} f_{\pm}(z, k) = 1 + \omega^{\pm}(z, k), \tag{1-3}$$

where  $ikz = ik(x_1 + ix_2)$  and  $\omega^{\pm}(z, k) = \mathcal{O}(1/|z|)$  as  $|z| \rightarrow \infty$ . Here  $z$  is considered as a spatial variable and  $k \in \mathbb{C}$  as a spectral parameter. We note that  $u = \text{Re } f_+$  satisfies (1-1), and denote  $\omega^{\pm}$  by  $\omega_{\mu}^{\pm}$  when emphasizing dependence on the Beltrami coefficient  $\mu$ . Recently, this technique has been generalized also for conductivities that are not in  $L^{\infty}(\Omega)$  but only exponentially integrable [Astala et al. 2016].

The two crucial ideas of the current work are:

- (i) To analyze the scattering series, we use the modified construction of Beltrami-CGO solutions of [Huhtanen and Perämäki 2012], which only involves exponentials of modulus 1 and where the solutions are constructed as a limit of an iteration of linear operations. This differs from the original construction of [Astala and Päivärinta 2006b], where the construction of the exponentially growing solutions is based on the Fredholm theorem.
- (ii) To transform the CGO solutions, we introduce polar coordinates in the spectral parameter  $k$ , followed by a partial Fourier transform in the radial direction.

These ideas are used as follows: Formally one can view the Beltrami equation (1-3) as a scattering equation, where  $\mu$  is considered as a compactly supported scatterer and the “incident field” is the constant function 1. Using (i), we write the CGO solutions  $\omega^{\pm}$  as a “scattering series”,

$$\omega^{\pm}(z, k) \sim \sum_{n=1}^{\infty} \omega_n^{\pm}(z, k), \tag{1-4}$$

considered as a formal power series (see Theorem 1.1)

Using (ii), we decompose  $k = \tau e^{i\varphi}$  and then, for each  $n$ , form the partial Fourier transform of the  $n$ -th order scattering term from (1-4) in  $\tau$ , denoting these by

$$\hat{\omega}_n^{\pm}(z, t, e^{i\varphi}) := \mathcal{F}_{\tau \rightarrow t}(\omega_n^{\pm}(z, \tau e^{i\varphi})). \tag{1-5}$$

As is shown in Section 5B, singularities in  $\sigma$  can be detected from averaged versions of  $\hat{\omega}_1^{\pm}$ , denoted by  $\hat{\omega}_1^{a,\pm}$ , formed by taking a complex contour integral of  $\hat{\omega}_1^{\pm}(z, t, e^{i\varphi})$  over  $z \in \partial\Omega$ ; see Figure 1.

Recall that the traces of CGO solutions  $\omega^{\pm}$  can be recovered perfectly from infinite-precision data  $\Lambda_{\sigma}$  [Astala and Päivärinta 2006a; 2006b]. When  $\sigma$  is close to 1, the single-scattering term  $\omega_1^{\pm}$  is close to  $\omega^{\pm}$ . Figure 1 suggests that what we can recover resembles parallel-beam X-ray projection data of the singularities of  $\mu$ . Indeed, we derive approximate reconstruction formulae for  $\mu$  (thus mildly nonlinear in  $\sigma$ ), analogous to the classical filtered back-projection method of X-ray tomography.

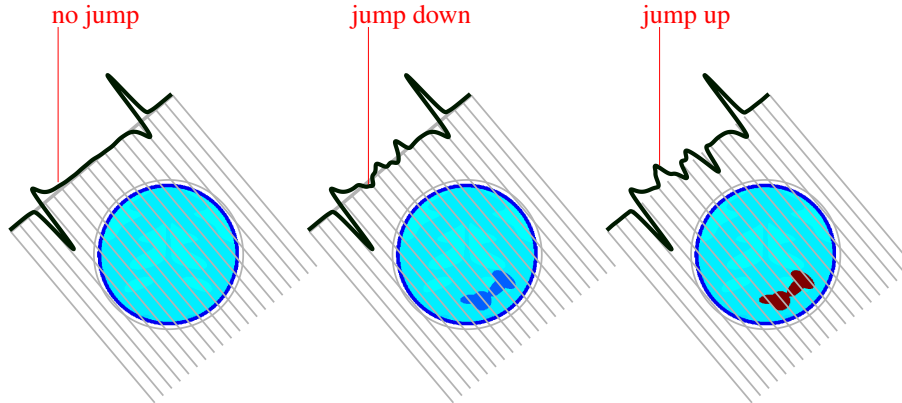


**Figure 1.** The method provides information about inclusions within inclusions in an unknown inhomogeneous background. Jump singularities in the conductivity show up in the function values much like in parallel-beam X-ray tomography: recording integrals along parallel lines over the coefficient function. This is illustrated using stroke-like computational phantoms. Left: Intact brain. Dark blue ring, with low conductivity, models the skull. Middle: Ischemic stroke, or blood clot preventing blood flow to the dark blue area. The conductivity in the affected area is less than that of the background. Right: Hemorrhagic stroke, or bleeding in the brain. The conductivity in the affected area is greater than the background. The function shown is  $T^{a,+}\mu(t/2, e^{i\varphi}) - T^{a,-}\mu(t/2, e^{i\varphi})$ , and  $\varphi$  indicates a direction perpendicular to the virtual “X-rays”.

The wave front sets of all of the terms  $\hat{\omega}_n^\pm$  are analyzed in Theorem 7.2. More detailed descriptions of the initial three terms,  $\hat{\omega}_1^\pm$ ,  $\hat{\omega}_2^\pm$  and  $\hat{\omega}_3^\pm$ , identifying the latter two as sums of paired Lagrangian distributions under a prior on the conductivity, are given in Section 5A, 6 and 9, respectively.

Let  $X = \{\mu \in L^\infty(\Omega) : \text{ess supp}(\mu) \subset \Omega_0, \|\mu\|_{L^\infty(\Omega)} \leq 1 - \epsilon\}$ , recalling that  $\Omega_0 \Subset \Omega$ . The expansion in (1-4) comes from the following:

**Theorem 1.1.** For  $k \in \mathbb{C}$ , define nonlinear operators  $W^\pm(\cdot; k) : X \rightarrow L^2(\Omega)$  by

$$W^\pm(\mu; k)(z) := \omega_\mu^\pm(z, k).$$

Then, at any  $\mu_0 \in X$ , we know  $W^\pm(\cdot; k)$  has Fréchet derivatives in  $\mu$  of all orders  $n \in \mathbb{N}$ , denoted by  $D^n W_k|_{\mu_0}$ , and the multiple scattering terms in (1-4) are given by

$$\omega_n^\pm = [D^n W_k^\pm(\mu, \mu, \dots, \mu)]|_{\mu=0}. \tag{1-6}$$

The  $n$ -th order scattering operators,

$$T_n^\pm : \mu \mapsto \hat{\omega}_n^\pm := \mathcal{F}_{\tau \rightarrow t}(\omega_n^\pm(z, \tau e^{i\varphi})), \quad z \in \partial\Omega, t \in \mathbb{R}, e^{i\varphi} \in \mathbb{S}^1, \tag{1-7}$$

which are homogeneous forms of degree  $n$  in  $\mu$ , have associated multilinear operators whose Schwartz kernels  $K_n$  have wave front relations which can be explicitly computed. See formulas (5-6) and (5-7) for

the case  $n = 1$  and (4-14) for  $n \geq 2$ .  $K_1$  is a Fourier integral distribution;  $K_2$  is a generalized Fourier integral (or paired Lagrangian) distribution; and for  $n \geq 3$ ,  $K_n$  has wave front set contained in a union of a family of  $2^{n-1}$  pairwise cleanly intersecting Lagrangians.

Singularity propagation for the first-order scattering  $\hat{\omega}_1^\pm$  is described by a Radon-type transform and a filtered back-projection formula; see [Kuchment 2014].

**Theorem 1.2.** Define averaged operators  $T_n^{a,\pm}$  for  $n \in \mathbb{N}$  and  $T^{a,\pm}$  by the complex contour integrals<sup>1</sup>

$$T_n^{a,\pm} \mu(t, e^{i\varphi}) = \frac{1}{2\pi i} \int_{\partial\Omega} \hat{\omega}_n^\pm(z, t, e^{i\varphi}) dz, \tag{1-8}$$

$$T^{a,\pm} \mu(t, e^{i\varphi}) = \frac{1}{2\pi i} \int_{\partial\Omega} \hat{\omega}^\pm(z, t, e^{i\varphi}) dz, \tag{1-9}$$

with  $\omega_n^\pm$  defined via formulas (1-6)–(1-7) and  $\omega^\pm$  defined via (1-3). Then we have

$$(-\Delta)^{-1/2} (T_1^{a,\pm})^* T_1^{a,\pm} \mu = \mu. \tag{1-10}$$

Theorem 1.2 suggests an approximate reconstruction algorithm:

- Given  $\Lambda_\sigma$ , follow [Astala et al. 2011, Section 4.1] to compute both  $\omega^+(z, k)$  and  $\omega^-(z, k)$  for  $z \in \partial\Omega$  by solving the boundary integral equation derived in [Astala and Päivärinta 2006a].
- Introduce polar coordinates in the spectral variable  $k$  and compute the partial Fourier transform,  $\hat{\omega}^\pm(z, t, e^{i\varphi})$ .
- Using the operator  $T^{a,\pm}$  defined in (1-9), we compute  $\tilde{\mu}^+ := \Delta^{-1/2} (T_1^{a,+})^* T^{a,+} \mu$  and  $\tilde{\mu}^- := \Delta^{-1/2} (T_1^{a,-})^* T^{a,-} \mu$ . Note the difference with (1-10).
- Approximately reconstruct by  $\sigma = (\mu - 1)/(\mu + 1) \approx (\tilde{\mu} - 1)/(\tilde{\mu} + 1)$ , where  $\tilde{\mu} = (\tilde{\mu}^+ - \tilde{\mu}^-)/2$ . The approximation comes from using  $T^{a,\pm} \mu$  instead of  $T_1^{a,\pm} \mu$  in the previous step.

See the middle column of Figure 2 for an example.

One can also use the identity  $(T_1^{a,\pm})^* T_1^{a,\pm} = (-\Delta)^{1/2}$  to enhance the singularities in the reconstruction. This is analogous to  $\Lambda$ -tomography in the context of linear X-ray tomography [Faridani et al. 1992; 1997]. See the right-most column in Figure 2 for reconstructions using the operator  $(T_1^{a,\pm})^* T^{a,\pm}$ .

Our general theorem on singularity propagation is quite technical, and so we illustrate it here using a simple example, postponing the precise statement and proof to Section 7 below.

Assume that the conductivity is of the form  $\sigma(z) = \sigma(|z|)$  and smooth except for a jump across the circle  $|z| = \rho$ . One can describe the singular supports of the  $\hat{\omega}_n^\pm(z, t, e^{i\varphi})$ . For  $m \in \mathbb{N}$ , define hypersurfaces

$$\Pi_m = \{(z, t, e^{i\varphi}) \in \mathbb{C} \times \mathbb{R} \times \mathbb{S}^1 : t = 2\rho m\}.$$

Using the analysis later in the paper, one can see that

$$(\text{sing supp}(\hat{\omega}_n^\pm) \cap \{(z, t, e^{i\varphi}); |z| \geq 1\}) \subset \bigcup \{\Pi_m : -n \leq m \leq n, m \equiv n \pmod{2}\}.$$

<sup>1</sup>Throughout,  $dz$  will denote the element of complex contour integration along a curve, while  $d^1x$  is arc length measure. We denote by  $d^2z$  two-dimensional Lebesgue measure in  $\mathbb{C}$ .

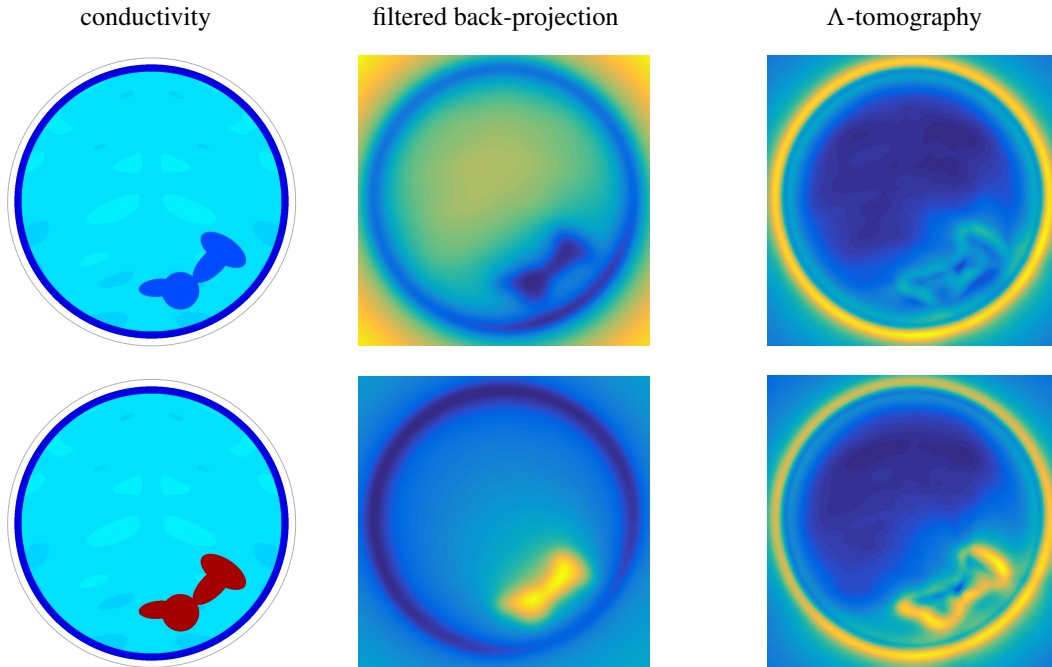


**Figure 2.** Reconstructions, of computational phantoms modeling ischemic strokes (top row) and hemorrhagic strokes (bottom row), from very high precision simulated EIT data. The results are promising for portable, cost-effective classification of strokes without use of ionizing radiation.

However, it turns out that, by a parity symmetry property described in Section 8, subtracting  $\hat{\omega}^-$  from  $\hat{\omega}^+$  eliminates the even terms,  $\hat{\omega}_{2n}^\pm$ , so that their singularities, including a strong one for  $\hat{\omega}_2^\pm$  at  $t = 0$ , do not create artifacts in the imaging. See Figure 3 for a diagram of singularity propagation in the case  $\rho = 0.2$ .

**1A. Ill-posedness, noise and deconvolution.** The exponential ill-posedness of the Calderón inverse problem (i.e., it satisfies a stability estimate of only logarithmic type) has important consequences for EIT with realistic data. Calderón inverse problems for elliptic equations were shown to be exponentially ill-posed in [Mandache 2001]. Corresponding to this, in [Knudsen et al. 2009, Lemma 2.4] it was shown that when the Dirichlet-to-Neumann map is given with error  $\epsilon$ , the boundary values of the CGO solutions, or equivalently,  $\omega(z, k)|_{z \in \partial\Omega}$ , can be found with accuracy  $\epsilon$  only for the frequencies  $|k| \leq R_\epsilon = c \log(\epsilon^{-1})$ .

This exponential instability holds even under the prior that conductivities consist of inclusions [Alessandrini and Di Cristo 2005]. Furthermore, inclusions need to have a minimum size to be detectable [Alessandrini 1988; Isaacson 1986; Cheney and Isaacson 1992], and in order to appear in reconstructions, the deeper inclusions are inside an object, the larger they must be [Nagayasu et al. 2009; Alessandrini and Scapin 2017; Garde and Knudsen 2017]. Finally, the resolution of reconstructions is limited by

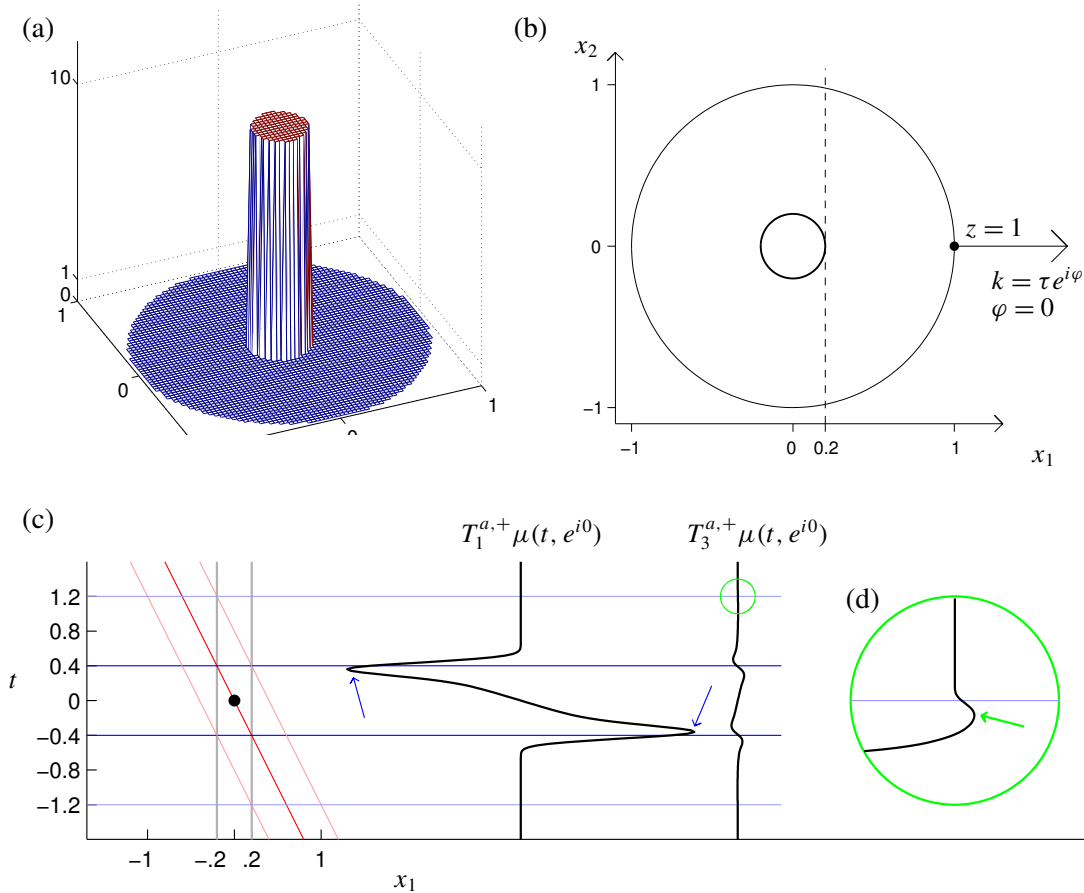


**Figure 3.** (a) Three-dimensional plot of the conductivity having a jump along the circle with radius  $\rho = 0.2$  and center at the origin. (b) Unit disc and singular support of the conductivity in the  $z$ -plane, where  $z = x_1 + ix_2$ . (c) The term  $T_1^{a,+} \mu(t, e^{i0})$  has peaks, indicated by blue arrows, at  $t = \pm 2\rho$  corresponding to the locations of the main singularities in  $\mu$ , as expected by Theorem 1.2. The higher-order term  $T_3^{a,+} \mu(t, e^{i0})$ , smaller than  $T_1^{a,+} \mu(t, e^{i0})$  in amplitude, exhibits singularities caused by reflections at both  $t = \pm 2\rho$  and  $t = \pm 6\rho$ . (d) The singularities of the term  $T_3^{a,+} \mu(t, e^{i0})$  at  $t = \pm 6\rho$  are very small. Shown is a zoom-in near  $t = 6\rho$ , with amplitude increased by a factor of 70.

noisy data. It is natural to ask how these limitations are reflected in the approach described in this paper.

Our results show that the part of the conductivity’s wave front set in the direction specified by  $\varphi$  is seen as specific singularities in the function  $\hat{\omega}^\pm(z, \cdot, e^{i\varphi})$ , defined in (1-5). However, due to algebraic decay of the principal symbol of a Fourier integral operator, the amplitude of the measured singularity is bounded by  $C \text{dist}(\partial\Omega, z)^{-1}$ , making it harder to recover details deep inside the imaging domain.

Furthermore, with realistic and noisy data, we can compute  $\omega^\pm(z, k)$  only in a disc  $|k| \leq k_{\max}$  with a measurement apparatus and noise-dependent radius  $k_{\max} > 0$ ; see [Knudsen et al. 2009; Astala et al.

2011; 2014]. With smaller noise we can take a larger  $k_{\max}$ , whereas large noise forces  $k_{\max}$  to be small. This makes it more difficult to locate singularities precisely.

To better understand the difficulty, consider the truncated Fourier transform:

$$\int_{-k_{\max}}^{k_{\max}} e^{-it\tau} \omega^{\pm}(z, \tau e^{i\varphi}) d\tau = \int_{-\infty}^{\infty} e^{-it\tau} \omega^{\pm}(z, \tau e^{i\varphi}) \chi_{k_{\max}}(\tau) d\tau, \quad (1-11)$$

where  $\chi_{k_{\max}}(\tau)$  is the characteristic function of the interval  $[-k_{\max}, k_{\max}]$ . Note that

$$\hat{\chi}_{k_{\max}}(t) = C \frac{\sin(k_{\max} t)}{t} \quad (1-12)$$

with a constant  $C \in \mathbb{R}$ . Noise forces us to replace the Fourier transform in (1-5) by a truncated integral such as (1-11). Therefore, we need to apply one-dimensional deconvolution in  $t$  to recover  $\hat{\omega}^{\pm}(z, \cdot, e^{i\varphi})$  approximately from  $\hat{\omega}^{\pm}(z, \cdot, e^{i\varphi}) * \hat{\chi}_{k_{\max}}$ . Higher noise level means a smaller  $k_{\max}$ , which by (1-12) leads to a wider blurring kernel  $\hat{\chi}_{k_{\max}}$ ; due to the Nyquist–Shannon sampling theorem, this results in a more ill-posed deconvolution problem and thus limits the imaging resolution.

In practice it is better to use a smooth windowing function instead of the characteristic function for reducing unwanted oscillations (Gibbs phenomenon), and there are many suitable deconvolution algorithms in the literature [Chen et al. 2001; Candès and Fernandez-Granda 2013; 2014].

It is also natural to ask how the method introduced here compares to previous work in terms of detecting inclusions and jumps.

Many methods have been proposed for regularized edge detection from EIT data. Examples include the *enclosure method* [Ikehata 2000; Ikehata and Siltanen 2000; 2004; Brühl and Hanke 2000; Ide et al. 2007; Uhlmann and Wang 2008], the *factorization method* [Kirsch 1998; Brühl and Hanke 2000; Lechleiter 2006; Lechleiter et al. 2008], the *monotonicity method* [Harrach and Ullrich 2013; 2015]. These methods can only detect the outer boundary of an inclusion in conductivity, whereas the method described here, which exploits the propagation of singularities for complex principal-type operators, can see nested jump curves. Also, the proposed method can deal with inclusions within inclusions, and with conductivities having both positive and negative jumps, even in unknown inhomogeneous smooth background.

One can also attempt edge detection based on EIT algorithms originally designed for reconstructing the full conductivity distribution. There are two main approaches: sharpening blurred EIT images in data-driven postprocessing [Hamilton et al. 2014; 2016], and applying sparsity-promoting inversion methods such as total variation regularization [Dobson and Santosa 1994; Kaipio et al. 2000; Rondi and Santosa 2001; Chan and Tai 2004; Chung et al. 2005; Tanushev and Vese 2007; van den Doel and Ascher 2006; Jin and Maass 2012; Garde and Knudsen 2016; Zhou et al. 2015]. As of now, the former approach does not have rigorous analysis available. Some of the latter kinds of approaches are theoretically capable of detecting nested inclusions; however, in variational regularization there is typically an instability issue, where a large low-contrast inclusion may be represented by a smaller high-contrast feature in the reconstruction. Numerical evidence suggests that method introduced here can accurately and robustly reconstruct jumps, both in terms of location and sign.

## 2. Complex principal-type structure of CGO solutions

We start by describing the microlocal geometry underlying the exponentially growing, or so-called *complex geometrical optics (CGO)*, solutions to the conductivity equation on  $\mathbb{R}^d$ ,  $d \geq 2$ ,

$$\nabla \cdot \sigma \nabla u(x) = 0, \quad x \in \mathbb{R}^n, \quad (2-1)$$

originating in [Sylvester and Uhlmann 1987]. For complex frequencies  $\zeta = \zeta_R + i\zeta_I \in \mathbb{C}^n$  with  $\zeta \cdot \zeta = 0$ , one can decompose  $\zeta$  as  $\zeta = \tau\eta$ , with  $\tau \in \mathbb{R}$  and  $\eta = \eta_R + i\eta_I$ ,  $|\eta_R| = |\eta_I| = 1$ ,  $\eta_R \cdot \eta_I = 0$ . Now consider solutions to (2-1) of the form

$$u(x) := e^{i\zeta \cdot x} w(x, \tau) = e^{i\tau\eta \cdot x} w(x, \tau).$$

Physically speaking,  $\tau$  can be considered as a spatial frequency, with the voltage on the boundary  $\partial\Omega$  oscillating at length scale  $\tau^{-1}$ .

The conductivity equation (2-1) becomes

$$\begin{aligned} 0 &= \frac{1}{\sigma} \nabla \cdot \sigma \nabla u(x) = \frac{1}{\sigma} \nabla \cdot \sigma \nabla (e^{i\tau\eta \cdot x} w(x, \tau)) \\ &= \left( \Delta + \left( \frac{1}{\sigma} \nabla \sigma \right) \cdot \nabla \right) (e^{i\tau\eta \cdot x} w(x, \tau)) \\ &= \left( \Delta w(x, \tau) + 2i\tau\eta \cdot \nabla w(x, \tau) + \left( \frac{1}{\sigma} \nabla \sigma \right) \cdot (\nabla + i\tau\eta) w(x, \tau) \right) e^{i\tau\eta \cdot x}. \end{aligned}$$

Hence, we have

$$\Delta w(x, \tau) + 2i\tau\eta \cdot \nabla w(x, \tau) + \left( \frac{1}{\sigma} \nabla \sigma \right) \cdot (\nabla + i\tau\eta) w(x, \tau) = 0.$$

Taking the partial Fourier transform  $\hat{w}$  in the  $\tau$ -variable and denoting the resulting dual variable by  $t$ , which can be thought of as a ‘‘pseudo-time’’, one obtains

$$\Delta \hat{w}(x, t) - 2\eta \frac{\partial}{\partial t} \cdot \nabla \hat{w}(x, t) + \left( \frac{1}{\sigma} \nabla \sigma \right) \cdot \left( \nabla - \eta \frac{\partial}{\partial t} \right) \hat{w}(x, t) = 0.$$

The principal part of this equation is given by the operator

$$\tilde{\square} = \mathcal{P}_R + i\mathcal{P}_I = \Delta - 2\eta \frac{\partial}{\partial t} \cdot \nabla,$$

where

$$\mathcal{P}_R = \Delta - 2\eta_R \frac{\partial}{\partial t} \cdot \nabla \quad \text{and} \quad \mathcal{P}_I = -2\eta_I \frac{\partial}{\partial t} \cdot \nabla.$$

With  $\xi$  the variable dual to  $x$ , the full symbols of  $\mathcal{P}_R$  and  $\mathcal{P}_I$  are

$$p_R(x, t, \xi, \tau) = -\xi^2 + 2\tau\eta_R \cdot \xi, \quad p_I(x, t, \xi, \tau) = 2\tau\eta_I \cdot \xi,$$

and these commute in the sense of Poisson brackets:  $\{p_R, p_I\} = 0$ . Furthermore, on the characteristic variety

$$\begin{aligned} \Sigma &:= \{(x, t, \xi, \tau) \in \mathbb{R}^{d+1} \times (\mathbb{R}^{d+1} \setminus \{0\}) : p_R(x, t, \xi, \tau) = 0, p_I(x, t, \xi, \tau) = 0\} \\ &= \{(x, t, \xi, \tau) \in \mathbb{R}^{d+1} \times (\mathbb{R}^{d+1} \setminus \{0\}) : |\xi|^2 - 2\tau\eta_R \cdot \xi = 0, 2\tau\eta_I \cdot \xi = 0\} \\ &= \{(x, t, \xi, \tau) \in \mathbb{R}^2 \times \mathbb{R} \times \mathbb{R}^2 \times (\mathbb{R} \setminus \{0\}) : \xi = 2\tau\eta_R \text{ or } \xi = 0\}, \end{aligned}$$

the gradients  $dp_R = (-2\xi + 2\tau\eta_R, 2\eta_R \cdot \xi)$  and  $dp_I = (2\tau\eta_I, 2\eta_I \cdot \xi)$  are linearly independent. Finally, no bicharacteristic leaf (see below) is trapped over a compact set. Thus,  $\tilde{\square} = \mathcal{P}_R + i\mathcal{P}_I$  is a *complex principal-type operator* in the sense of [Duistermaat and Hörmander 1972].

Recall that for a *real* principal-type operator, such as  $\partial/\partial x_1$  in  $\mathbb{R}^m$ ,  $m \geq 2$ , or the d'Alembertian wave operator, the singularities propagate along curves (the characteristics); for instance, for the wave equation, singularities propagate along light rays. *Complex* principal-type operators, such as  $\partial_{x_1} + i\partial_{x_2}$  in  $\mathbb{R}^m$ ,  $m \geq 3$ , or the operator  $\tilde{\square}$  above, also propagate singularities, but now along *two-dimensional* surfaces, called leaves, which are the spatial projections of the bicharacteristic surfaces formed by the joint flowout of  $H_{p_R}, H_{p_I}$ . For the operator  $\tilde{\square}$  above, this roughly means that if  $\tilde{\square}\hat{w}(x, t) = \hat{f}(x, t)$  and  $(x_0, t_0, \xi_0, \tau_0) \in \Sigma$  is in the wave front set of  $\hat{f}(x, t)$ , then the wave front set of  $\hat{w}(x, t)$  contains a plane through this point. See [Duistermaat and Hörmander 1972, Section 7.2] for detailed statements.

In the situation relevant for this paper, the  $x$ -projection of any bicharacteristic leaf is all of  $\mathbb{R}^2$  and thus reaches all points of  $\bar{\Omega}$ . Thus, complete information about  $\sigma$  in the interior is accessible to boundary measurements made at *any* point on  $\partial\Omega$ . We will see below that although this is the case, using suitable weighted integrals over the boundary produces far superior imaging; however, this is due to the amplitudes, not the underlying geometry.

For the remainder of the paper, we limit ourselves to the Calderón problem in  $\mathbb{R}^2$ ; we begin by recalling the complex Beltrami equation formalism and CGO solutions of [Astala and Päivärinta 2006b], as well as their modification in [Huhtanen and Perämäki 2012]. The complex analysis in these approaches reflects the complex principal-type structure discussed above, disguised by the fact that we are working in two dimensions.

### 3. Conductivity equations and CGO solutions

On a domain  $\Omega \subset \mathbb{R}^2 = \mathbb{C}$ , let  $\sigma \in L^\infty(\Omega)$  be a strictly positive conductivity,  $\sigma \equiv 1$  near  $\partial\Omega$ , and extended to be  $\equiv 1$  outside of  $\Omega$ . The complex frequencies  $\zeta \in \mathbb{C}^2$  with  $\zeta \cdot \zeta = 0$  may be parametrized by  $\zeta = (k, ik)$ ,  $k \in \mathbb{C}$ ; thus, with  $z = x_1 + ix_2$ , one has  $\zeta \cdot x = kz$ . Following [Astala and Päivärinta 2006b], consider simultaneously the conductivity equations for the two scalar conductivities  $\sigma$  and  $\sigma^{-1}$ ,

$$\nabla \cdot \sigma \nabla u_1 = 0, \quad u_1 \sim e^{ikz}, \tag{3-1}$$

$$\nabla \cdot \sigma^{-1} \nabla u_2 = 0, \quad u_2 \sim e^{ikz}. \tag{3-2}$$

The complex geometrical optics (CGO) solutions of [Astala and Päivärinta 2006b], see also [Astala et al. 2010; 2014; Brown and Uhlmann 1997; Caro and Rogers 2016; Greenleaf and Uhlmann 2001; Haberman 2015; Haberman and Tataru 2013; Hamilton et al. 2012; Knudsen 2003; Knudsen et al. 2007; Nachman 1996], are specified by their asymptotics  $u_j \sim e^{ikz}$ , meaning that for all  $k \in \mathbb{C}$ ,

$$u_j(z, k) = e^{ikz} \left( 1 + \mathcal{O}\left(\frac{1}{z}\right) \right) \quad \text{as } |z| \rightarrow \infty. \tag{3-3}$$

The CGO solutions are constructed via the Beltrami equation

$$\bar{\partial}_z f_\mu = \mu \overline{\partial_z f_\mu}, \tag{3-4}$$

where the Beltrami coefficient  $\mu$  is defined in terms of  $\sigma$  by

$$\mu := \frac{1 - \sigma}{1 + \sigma}. \tag{3-5}$$

The Beltrami coefficient  $\mu$  is a compactly supported,  $(-1, 1)$ -valued function and, due to the assumption that  $0 < c_1 \leq \sigma \leq c_2 < \infty$ , one has  $|\mu| \leq 1 - \epsilon$  for some  $\epsilon > 0$ . It was shown in [Astala and Päivärinta 2006b] that (3-4) has solutions for coefficients  $\mu$  and  $-\mu$  of the form

$$f_\mu(z, k) = e^{ikz}(1 + \omega^+(z, k)) \quad \text{and} \quad f_{-\mu}(z, k) = e^{ikz}(1 + \omega^-(z, k)), \tag{3-6}$$

with

$$\omega^\pm(z, k) = \mathcal{O}\left(\frac{1}{|z|}\right) \quad \text{as } |z| \rightarrow \infty.$$

The various CGO solutions are then related by the equation

$$2u_1(z, k) = f_\mu(z, k) + f_{-\mu}(z, k) + \overline{f_\mu(z, \bar{k})} - \overline{f_{-\mu}(z, \bar{k})}, \tag{3-7}$$

which follows from the fact that the real part of  $f_\mu(z, k)$  solves (3-1), while the imaginary part solves (3-2).

In this work we will mainly focus on  $\omega^+$ , henceforth denoted simply by  $\omega$ ; however, we will use  $\omega^-$  in the symmetry discussion in Section 8. Both of these can be extracted from voltage/current measurements for  $\sigma$  at the boundary,  $\partial\Omega$ , as encoded in the Dirichlet-to-Neumann (DN) map of (3-1). For the most part we will suppress the superscripts  $\pm$ , with it being understood in the formulas that for  $\omega^\pm$ , one uses  $\pm\mu$ .

Huhtanen and Perämäki [2012] introduced the following modified derivation of  $\omega$ , which, by avoiding issues caused by the exponential growth in the  $k^\perp$ -directions, is highly efficient from a computational point of view.

Let  $e_k(z) := \exp(i(kz + \bar{k}\bar{z})) = \exp(i2 \operatorname{Re}(kz))$ ; note that  $|e_k(z)| \equiv 1$  and  $\bar{e}_k = e_{-k}$ . Define, as in [Astala and Päivärinta 2006a; 2006b],

$$v(z, k) := e_{-k}(z)\mu(z) \quad \text{and} \quad \alpha(z, k) := -i\bar{k}e_{-k}(z)\mu(z). \tag{3-8}$$

Both  $\alpha$  and  $v$  are compactly supported in  $\Omega$ ; since  $\bar{\partial}\omega = v\bar{\partial}\bar{\omega} + \alpha\bar{\omega} + \alpha$ , we see that  $\bar{\partial}\bar{\omega}$  is compactly supported as well. For future use, also note that

$$\bar{v}(z, k) = e_k(z)\mu(z) \quad \text{and} \quad \bar{\alpha}(z, k) = ike_k(z)\mu(z). \tag{3-9}$$

Astala and Päivärinta [2006b, (4.8)] showed that  $\omega(z, k)$  satisfies the inhomogeneous Beltrami equation

$$\bar{\partial}\omega - v\bar{\partial}\bar{\omega} - \alpha\bar{\omega} = \alpha, \tag{3-10}$$

where the Cauchy–Riemann operator  $\bar{\partial}$  and derivative  $\partial$  are taken with respect to  $z$ . Recall the (solid) Cauchy transform  $P$  and Beurling transform  $S$ , defined by

$$Pf(z) = -\frac{1}{\pi} \int_{\mathbb{C}} \frac{f(z_1)}{z_1 - z} d^2z_1, \tag{3-11}$$

$$Sg(z) = -\frac{1}{\pi} \int_{\mathbb{C}} \frac{g(z_1)}{(z_1 - z)^2} d^2z_1, \tag{3-12}$$

which satisfy  $\bar{\partial}P = I$ ,  $S = \partial P$  and  $S\bar{\partial} = \partial$  on  $C_0^\infty(\mathbb{C})$ ; see [Astala et al. 2009].

It is shown in [Huhtanen and Perämäki 2012], using the results of [Astala and Päiväranta 2006b], that (3-10) has a unique solution  $\omega \in W^{1,p}(\mathbb{C})$  for  $2 < p < p_\epsilon := 1 + 1/(1 - \epsilon)$ , where  $\epsilon > 0$  is such that  $|\mu| \leq 1 - \epsilon$ . Now define  $u$  on  $\Omega$  by  $\bar{u} = -\bar{\partial}\omega$ ; note that  $u \in L^p(\Omega)$ ,  $\omega = -P\bar{u}$  and  $\partial\omega = -S\bar{u}$ . Rewriting (3-10) in terms of  $u$  leads to

$$-\bar{u} - v(\overline{-S\bar{u}}) - \alpha(\overline{-P\bar{u}}) = \alpha.$$

Using (3-8), this further simplifies to

$$u + (-\bar{v}S - \bar{\alpha}P)\bar{u} = -\bar{\alpha}, \quad (3-13)$$

which then can be expressed as the integral equation

$$(I + A\rho)u = -\bar{\alpha}, \quad (3-14)$$

where  $\rho(f) := \bar{f}$  denotes complex conjugation and  $A := (-\bar{\alpha}P - \bar{v}S)$ . As shown in [Astala and Päiväranta 2006b, Huhtanen and Perämäki 2012, Section 2],  $I + A$  is invertible on  $L^p(\Omega)$ . Denote by  $U(k, \mu) = u(\cdot, k)|_{\bar{\Omega}}$  the restriction to  $\bar{\Omega}$  of the unique solution to (3-14), and hence (3-13).

#### 4. Fréchet differentiability and the Neumann series

We now come to the key construction of the paper. For  $\epsilon > 0$  and any  $\Omega_0 \Subset \Omega$ , let

$$X = \{\mu \in L^\infty(\Omega) : \text{ess supp}(\mu) \subset \Omega_0, \|\mu\|_{L^\infty(\Omega)} \leq 1 - \epsilon\}.$$

Furthermore, define  $Y$  to be the closure of  $C^\infty(\bar{\Omega})$  with respect to

$$\|u\|_Y := \|u\|_{L^2(\Omega)} + \|u|_{\partial\Omega}\|_{L^\infty(\partial\Omega)}.$$

For  $k \in \mathbb{C}$ , let  $U_k$  be the  $\mathbb{R}$ -linear map  $U_k : X \rightarrow L^2(\Omega)$ , given by  $U_k(\mu) = u_\mu(\cdot, k)$ , where  $u_\mu(z, k)$  is the unique solution  $u = u_\mu(\cdot, k) \in L^2(\Omega)$  of (3-13). Define  $W_k : X \rightarrow Y$  by

$$W_k\mu = \omega_\mu(\cdot, k) = -P(\overline{u_\mu(\cdot, k)}).$$

**4A. Fréchet differentiability.** We will show that, for each  $k \in \mathbb{C}$ ,  $W_k$  is a  $C^\infty$ -map  $X \rightarrow Y$  and analyze its Fréchet derivatives at  $\mu_0 = 0$ . For each  $k$ , one can solve (3-14) by a Neumann series which converges for  $\|\mu\|_{L^\infty}$  sufficiently small. We analyze the individual terms of the series by introducing polar coordinates in the  $k$ -plane,  $k = \tau e^{i\varphi}$ , and then taking the partial Fourier transform in  $\tau$ . The leading term in the Neumann series will be the basis for the edge-detection imaging technique that is the main point of the paper, while the higher-order terms are transformed into multilinear operators acting on  $\mu$ . The remainder of the paper will then be devoted to understanding the Fourier-transformed terms, using the first derivative for effective edge detection in EIT and obtaining partial control over the higher derivatives.

**Theorem 4.1.** *The map  $U_k : X \rightarrow L^2(\Omega)$ ,  $U_k(\mu) := u_\mu(\cdot, k)$ , is infinitely Fréchet-differentiable with respect to  $\mu$ , and its Fréchet derivatives are real-analytic functions of  $k \in \mathbb{C}$ . Moreover, for  $p \geq 1$ , its  $p$ -th order Fréchet derivative at  $\mu = 0$  in the direction  $(\mu_1, \mu_2, \dots, \mu_p) \in (L^2(\Omega_0))^p$  satisfies*

$$\left\| \frac{D^p U_k}{D\mu^p} \Big|_{\mu=0} (\mu_1, \mu_2, \dots, \mu_p) \right\|_{L^2(\Omega)} \leq C_p (1 + |k|)^p \|\mu_1\|_{L^2(\Omega)} \cdot \|\mu_2\|_{L^2(\Omega)} \cdots \|\mu_p\|_{L^2(\Omega)} \quad (4-1)$$

for some  $C_p > 0$ . In particular, the first Fréchet derivative has the form

$$\frac{DU_k}{D\mu} \Big|_{\mu=0} (\mu_1) = -P\rho(ike_{-k}\mu_1). \tag{4-2}$$

Moreover, for  $k \in \mathbb{C}$  the map  $W_k : X \rightarrow Y$ ,

$$W_k(\mu) := \omega_\mu(\cdot, k) = -P\rho(u_\mu(\cdot, k)),$$

is infinitely Fréchet-differentiable with respect to  $\mu$  and its Fréchet derivatives are real-analytic functions of  $k \in \mathbb{C}$ .

*Proof.* We can rewrite (3-13) for  $u = u_\mu(\cdot, k) \in L^2(\Omega)$  as

$$(I - e_k\mu S\rho)u + ike_k\mu P\rho u = ike_k\mu. \tag{4-3}$$

On the left-hand side,  $e_k$  and  $\mu$  denote pointwise multiplication operators with the functions  $e_k(z)$  and  $\mu(z)$ , respectively; on the right,  $e_k(z)\mu(z)$  is an element of  $L^2(\Omega)$ .

Since  $\|\rho\|_{L^2(\Omega) \rightarrow L^2(\Omega)} = 1$ ,  $\|S\|_{L^2(\Omega) \rightarrow L^2(\Omega)} = 1$ , and  $\|\mu\|_{L^\infty(\Omega)} < 1$ , the inverse operator  $(I - e_k\mu S\rho)^{-1} : L^2(\Omega) \rightarrow L^2(\Omega)$  exists and is a  $C^\omega$  function (i.e., a real analytic function) of  $k$ . Thus, (4-3) can be rewritten as

$$(I - B_{\mu,k})u = K_{\mu,k}(ike_k\mu), \tag{4-4}$$

where

$$K_{\mu,k}u = (I - e_k\mu S\rho)^{-1}u, \quad B_{\mu,k}u = K_{\mu,k}(ike_k\mu P\rho u). \tag{4-5}$$

Since  $P : L^2(\Omega) \rightarrow L^2(\Omega)$  is a compact operator, (4-5) defines a compact operator  $B_{\mu,k} : L^2(\Omega) \rightarrow L^2(\Omega)$ . To find the kernel of  $I - B_{\mu,k}$ , consider  $u^0 \in L^2(\Omega)$  satisfying  $(I - B_{\mu,k})u^0 = 0$ . Then,

$$(I - e_k\mu S\rho)u^0 + ike_k\mu P\rho u^0 = 0. \tag{4-6}$$

When we consider  $P$ , given in (3-11), as an operator  $P : L^2(\Omega) \rightarrow L^2_{\text{loc}}(\mathbb{C})$ , equation (4-6) yields that  $f^0(z) = -e^{ikz}(P\bar{u})(z) \in L^2_{\text{loc}}(\mathbb{C})$  satisfies

$$\begin{aligned} \bar{\partial}_z f^0(z) &= \mu(z) \overline{\partial_z f^0(z)}, \quad z \in \mathbb{C}, \\ e^{-ikz} f^0(z) &= \mathcal{O}\left(\frac{1}{|z|}\right) \quad \text{as } |z| \rightarrow \infty. \end{aligned} \tag{4-7}$$

By [Astala and Päiväranta 2006b], the solution  $f^0$  of (4-7) has to be zero. Hence,

$$u^0(z) = -\overline{\partial(e^{-ikz} f^0(z))} = 0$$

and the operator  $I - B_{\mu,k} : L^2(\Omega) \rightarrow L^2(\Omega)$  is one-to-one. Thus the Fredholm equation (4-4) is uniquely solvable and we can write its solutions as  $u = u_\mu(\cdot, k)$ ,

$$u_\mu(\cdot, k) = (I - B_{\mu,k})^{-1}K_{\mu,k}(ike_k\mu). \tag{4-8}$$

By the analytic Fredholm theorem, the maps  $k \mapsto K_{\mu,k}$  and  $k \mapsto (I - B_{\mu,k})^{-1}$  are real-analytic,  $\mathbb{C} \rightarrow \mathcal{L}(L^2(\Omega), L^2(\Omega))$ , where  $\mathcal{L}(L^2(\Omega), L^2(\Omega))$  is the space of the bounded linear operators  $L^2(\Omega) \rightarrow L^2(\Omega)$ .

Define

$$K^{(p)} = \frac{D^p}{D\mu^p} K_{\mu,k} \Big|_{\mu=0} \quad \text{and} \quad B^{(p)} = \frac{D^p}{D\mu^p} B_{\mu,k} \Big|_{\mu=0}.$$

Since  $K_{\mu,k}|_{\mu=0} = I$ , we see that

$$K^{(p)}(\mu_1, \mu_2, \dots, \mu_p) = \sum_{\sigma} (e_k \mu_{\sigma(1)} S\rho) \circ (e_k \mu_{\sigma(2)} S\rho) \circ \dots \circ (e_k \mu_{\sigma(p)} S\rho),$$

where the sum is taken over permutations  $\sigma : \{1, 2, \dots, p\} \rightarrow \{1, 2, \dots, p\}$ . Furthermore, one has

$$\begin{aligned} B^{(p)}(\mu_1, \mu_2, \dots, \mu_p) &= K^{(p-1)}(\mu_2, \mu_3, \mu_4, \dots, \mu_p) \circ (ike_k \mu_1 P\rho) \\ &\quad + K^{(p-1)}(\mu_1, \mu_3, \mu_4, \dots, \mu_p) \circ (ike_k \mu_2 P\rho) \\ &\quad + K^{(p-1)}(\mu_1, \mu_2, \mu_4, \dots, \mu_p) \circ (ike_k \mu_3 P\rho) \\ &\quad + \dots + K^{(p-1)}(\mu_1, \mu_2, \dots, \mu_{p-1}) \circ (ike_k \mu_p P\rho). \end{aligned}$$

We can compute the higher-order derivatives

$$\frac{D^p}{D\mu^p} (I - B_{\mu,k})^{-1} \Big|_{\mu=0},$$

in the direction  $(\mu_1, \mu_2, \dots, \mu_p)$ , using the polarization identity for symmetric multilinear functions, if these derivatives are known in the case when  $\mu_1 = \mu_2 = \dots = \mu_p$ . In the latter case the derivatives can be computed using Faà di Bruno’s formula, which generalizes the chain rule to higher derivatives,

$$\frac{d^p}{dt^p} f(g(t)) = \sum \frac{p!}{m_1! m_2! \dots m_p!} \cdot f^{(m_1+\dots+m_p)}(g(t)) \cdot \prod_{j=1}^n \left( \frac{g^{(j)}(t)}{j!} \right)^{m_j},$$

where the sum runs over indices  $(m_1, m_2, \dots, m_p) \in \mathbb{N}^p$  satisfying  $m_1 + 2m_2 + \dots + pm_p = p$ . Indeed, this formula can be applied with  $f(B) = (I - B)^{-1}$  and  $g(t) = B_{t\mu_1,k}$ . As  $g(0) = 0$  and the norm of the  $p$ -th derivative of  $B_{t\mu_1,k}$  with respect to  $t$  is bounded by  $c_p(1 + |k|)^p \|\mu_1\|^p$ , we obtain estimate (4-1). Moreover, since  $k \mapsto ik e_k \mu$  is a real analytic map,  $\mathbb{C} \rightarrow L^2(\Omega)$ , we see that the Fréchet derivatives

$$k \mapsto \frac{D^p u_{\mu}}{D\mu^p} \Big|_{\mu=0} (\cdot, k) \in L^2(\Omega)$$

are real analytic maps of  $k \in \mathbb{C}$ .

Finally, recall that  $\Omega_0 \subset \Omega$  is a relatively compact set. For  $\mu \in X$ , we have  $\text{supp}(\mu) \subset \Omega_0$ , and thus the function  $u_{\mu}(\cdot, k) = U_k(\mu)$  is also supported in  $\Omega_0$ . As  $P$  is given in (3-11) we see easily that for  $(\mu_1, \mu_2, \dots, \mu_p) \in (L^2(\Omega_1))^p$  the Fréchet derivatives

$$\frac{D^p W_k}{D\mu^p} \Big|_{\mu=0} (\mu_1, \mu_2, \dots, \mu_p) = -P\rho \frac{D^p U_k}{D\mu^p} \Big|_{\mu=0} (\mu_1, \mu_2, \dots, \mu_p)$$

are in  $Y$ , and these derivatives are real analytic functions of  $k \in \mathbb{C}$ . □

**4B. Neumann series.** Now consider a Neumann-series-expansion approach to solving (3-14), looking for  $u \sim \sum_{n=1}^{\infty} u_n$ , with  $u_1 := -\bar{\alpha}$  and  $u_{n+1} := -A\bar{u}_n$ ,  $n \geq 1$ ; the resulting  $\omega_n$  are defined by

$$\omega = -P\bar{u} \sim \sum_{n=1}^{\infty} -P\bar{u}_n =: \sum_{n=1}^{\infty} \omega_n.$$

The first three terms of each expansion are given by

$$u_1 = -\bar{\alpha}, \quad \omega_1 = P\alpha, \quad (4-9)$$

$$u_2 = A\alpha = -(\bar{\alpha}P + \bar{v}S)(\alpha), \quad \omega_2 = P(\alpha\bar{P}\bar{\alpha} + v\bar{S}\bar{\alpha}), \quad (4-10)$$

$$u_3 = -(\bar{\alpha}P + \bar{v}S)(\alpha\bar{P}\bar{\alpha} + v\bar{S}\bar{\alpha}), \quad \omega_3 = P(\alpha\bar{P} + v\bar{S})(\bar{\alpha}P\alpha + \bar{v}S\alpha). \quad (4-11)$$

By Theorem 4.1,  $U_k : X \rightarrow L^2(\Omega)$  is  $C^\infty$ , and hence we have

$$u_n(\cdot, k) = \frac{D^n U_k}{D\mu^n} \Big|_{\mu_0=0} (\mu, \mu, \dots, \mu), \quad \omega_n(\cdot, k) = -P\rho(u_n(\cdot, k)). \quad (4-12)$$

Due to the polynomial growth in the estimates (4-1), the functions  $u_n(z, k)$  and  $\omega_n(z, k)$  are tempered distributions in the  $k$ -variable. Hence we can introduce polar coordinates,  $k = \tau e^{i\varphi}$ , and then take the partial Fourier transform with respect to  $\tau$  of the tempered distributions  $\tau \mapsto u_n(z, k)|_{k=\tau e^{i\varphi}}$  and  $\tau \mapsto \omega_n(z, k)|_{k=\tau e^{i\varphi}}$ . Later we prove the following theorem concerning the partial Fourier transforms of the Fréchet derivatives:

**Theorem 4.2.** *Let  $\mu \in X$  and consider the partial Fourier transforms of the Fréchet derivatives*

$$\begin{aligned} \hat{\omega}_n^{z_0}(t, e^{i\varphi}) &= \mathcal{F}_{\tau \rightarrow t}(\omega_n(z_0, k)|_{k=\tau e^{i\varphi}}), \quad n = 1, 2, \dots, \\ \omega_n(\cdot, k) &= -P\rho\left(\frac{D^{n+1}U_k}{D\mu^{n+1}} \Big|_{\mu_0=0} (\mu, \mu, \dots, \mu)\right), \end{aligned} \quad (4-13)$$

which we denote at  $z_0 \in \partial\Omega$  by

$$\hat{\omega}_n(z_0, t, e^{i\varphi}) = \hat{\omega}_n^{z_0}(t, e^{i\varphi}).$$

Then we have

$$\hat{\omega}_n^{z_0}(t, e^{i\varphi}) = T_n^{z_0}(\mu \otimes \dots \otimes \mu),$$

where  $T_n^{z_0}$  are  $n$ -linear operators given by

$$T_n^{z_0}(\mu_1 \otimes \dots \otimes \mu_n) := \int_{\mathbb{C}^n} K_n^{z_0}(t, e^{i\varphi}; z_1, \dots, z_n) \mu_1(z_1) \dots \mu_n(z_n) d^2z_1 \dots d^2z_n.$$

The wave front set of the Schwartz kernel  $K_n^{z_0}$  is contained in the union of a collection  $\{\Lambda_J : J \in \mathcal{J}\}$  of  $2^{n-1}$  pairwise cleanly intersecting Lagrangian manifolds, indexed by  $\mathcal{J}$ , the power set of  $\{1, \dots, n-1\}$ . For each  $J \in \mathcal{J}$ , we have  $\Lambda_J$  is the conormal bundle of a smooth submanifold,  $L_n^J \subset \mathbb{R} \times \mathbb{S}^1 \times \mathbb{C}^n$ , i.e.,  $\Lambda_J = N^*L_n^J$ , with

$$L_n^J := \left\{ t + (-1)^{n+1} 2 \operatorname{Re} \left( e^{i\varphi} \sum_{j=1}^n (-1)^j z_j \right) = 0 \right\} \cap \bigcap_{j \in J} \{z_j - z_{j+1} = 0\}. \quad (4-14)$$

Roughly speaking, Theorem 4.2 implies that the operator  $T_n^{z_0}$  transforms singularities of  $\mu$  to singularities of  $\hat{\omega}_n^{z_0}$  so that the singularities of  $\mu$  propagate along the  $L_n^J$ . Further discussion, as well as the proof of the theorem, will be found later in the paper.

The first-order term  $\omega_1$  will serve as the basis for stable edge and singularity detection, while the higher-order terms need to be characterized in terms their regularity and the location of their wave front sets. After the partial Fourier transform  $\omega \rightarrow \hat{\omega}$  described in the next section, the map  $T_1 : \mu \rightarrow \hat{\omega}_1$  turns out to be essentially a derivative of the Radon transform. Thus, *the leading term of  $\hat{\omega}$  is a nonlinear Radon transform* of the conductivity  $\sigma$ , allowing for good reconstruction of the singularities of  $\sigma$  from the singularities of  $\hat{\omega}_1$ . The higher-order terms  $\hat{\omega}_n$  record scattering effects and explain artifacts observed in simulations; these should be filtered out or otherwise taken into account for efficient numerics and accurate reconstruction. We characterize this scattering in detail for  $\hat{\omega}_2$  in terms of oscillatory integrals, almost as precisely for  $\hat{\omega}_3$ , and in terms of the wave front set for  $\hat{\omega}_n$ ,  $n \geq 4$ .

**5. Fourier transform and the virtual variable**

We continue the analysis with two elementary transformations of the problem:

- (i) First, one introduces polar coordinates in the complex frequency,  $k$ , writing  $k = \tau e^{i\varphi}$ , with  $\tau \in \mathbb{R}$  and  $e^{i\varphi} \in \mathbb{S}^1$ .
- (ii) Secondly, one takes a partial Fourier transform in  $\tau$ , introducing a nonphysical artificial (i.e., *virtual*) variable,  $t$ . We show that the introduction of this variable reveals the complex principal-type structure of the problem, as discussed in Section 2. This allows for good propagation of singularities from the interior of  $\Omega$  to the boundary, allowing singularities of the conductivity in the interior to be robustly detected by voltage-current measurements at the boundary.

By (3-8),  $\omega_1 = ikP(e_k\mu)$ , see also (4-2), so that

$$\omega_1(z, k) = \frac{ik}{\pi} \int_{\mathbb{C}} \frac{e_k(z_1)\mu(z_1)}{z - z_1} d^2z_1. \tag{5-1}$$

Write the complex frequency as  $k = \tau e^{i\varphi}$  with  $\tau \in \mathbb{R}$ ,  $\varphi \in [0, 2\pi)$  (which we usually identify with  $e^{i\varphi} \in \mathbb{S}^1$ ). Taking the partial Fourier transform in  $\tau$  then yields

$$\begin{aligned} \hat{\omega}_1(z, t, e^{i\varphi}) &:= \int_{\mathbb{R}} e^{-it\tau} \omega_1(z, \tau e^{i\varphi}) d\tau \\ &= \frac{e^{i\varphi}}{\pi} \int_{\mathbb{R}} \int_{\mathbb{C}} \frac{e^{-i\tau t}}{z - z_1} (i\tau) e_{\tau e^{i\varphi}}(z_1)\mu(z_1) d^2z_1 d\tau \\ &= \frac{e^{i\varphi}}{\pi} \int_{\mathbb{R}} \int_{\mathbb{C}} (i\tau) \frac{e^{-i\tau(t - 2\operatorname{Re}(e^{i\varphi}z_1))}}{z - z_1} \mu(z_1) d^2z_1 d\tau \\ &= -2e^{i\varphi} \int_{\mathbb{C}} \frac{\delta'(t - 2\operatorname{Re}(e^{i\varphi}z_1))}{z - z_1} \mu(z_1) d^2z_1, \end{aligned} \tag{5-2}$$

with the integrals interpreted in the sense of distributions. Note that since  $t$  is dual to  $\tau$ , which is the (signed) length of a frequency variable, for heuristic purposes  $t$  may be thought of as temporal.

**5A. Microlocal analysis of  $\hat{\omega}_1$ .** Fix  $\Omega_0 \Subset \Omega_2 \Subset \Omega$  and assume once and for all that  $\text{supp}(\mu) \subset \Omega_0$ , i.e.,  $\sigma \equiv 1$  on  $\Omega_0^c$ . Let  $\Omega_1 := (\overline{\Omega_2})^c \supset \Omega^c \supset \partial\Omega$ . Then the map  $T_1 : \mathcal{E}'(\Omega_0) \rightarrow \mathcal{D}'(\Omega_1 \times \mathbb{R} \times \mathbb{S}^1)$ , defined by

$$\mu(z_1) \rightarrow (T_1\mu)(z, t, e^{i\varphi}) := \hat{\omega}_1(z, t, e^{i\varphi}),$$

has Schwartz kernel

$$K_1(z, t, e^{i\varphi}, z_1) = -2e^{i\varphi} \frac{\delta'(t - 2 \operatorname{Re}(e^{i\varphi} z_1))}{z - z_1}. \tag{5-3}$$

Note that  $|z - z_1| \geq c > 0$  for  $z \in \Omega_1$  and  $z_1 \in \Omega_0$ . For  $z \in \partial\Omega$  and  $z_1 \in \Omega_0$ , the factor  $(z - z_1)^{-1}$  in (5-3) is smooth, and  $T_1$  acts on  $\mu \in \mathcal{E}'(\Omega_0)$  as a standard Fourier integral operator (FIO). (See [Hörmander 1971] for the standard facts concerning FIOs which we use.) However, as we will see below, the amplitude  $1/(z - z_1)$ , although  $C^\infty$ , both

- (i) accounts for the fall-off rate in detectability of jumps, namely as the inverse of the distance from the boundary; and
- (ii) causes artifacts, especially when some singularities of  $\mu$  are close to the boundary, due to its large magnitude and the large gradient of its phase.

To see this, start by noting that the kernel  $K_1$  is singular at the hypersurface,

$$L := \{(z, t, e^{i\varphi}, z_1) : t - 2 \operatorname{Re}(e^{i\varphi} z_1) = 0\} \subset \mathbb{C} \times \mathbb{R} \times \mathbb{S}^1 \times \mathbb{C}.$$

Write  $z = x + iy$ ,  $z_1 = x' + iy'$ , and use  $\zeta, \zeta'$  to denote their dual variables,  $(\xi, \eta), (\xi', \eta')$ . Using the defining function  $t - 2 \operatorname{Re}(e^{i\varphi} z_1) = t - 2(\cos(\varphi)x' - \sin(\varphi)y')$ , identifying  $\mathbb{C}$  with  $\mathbb{R}^2$  as above and  $\mathbb{S}^1$  with  $[0, 2\pi)$ , we see that the conormal bundle of  $L$  is

$$\Lambda := N^*L = \{(z, 2 \operatorname{Re}(e^{i\varphi} z_1), e^{i\varphi}, x', y'; 0, 0, \tau, 2\tau \operatorname{Im}(e^{i\varphi} z_1), -2\tau e^{-i\varphi}) : z \in \Omega_1, z_1 \in \Omega_0, e^{i\varphi} \in \mathbb{S}^1, \tau \in \mathbb{R} \setminus \{0\}\}, \tag{5-4}$$

which is a Lagrangian submanifold of  $T^*(\Omega_1 \times \mathbb{R} \times \mathbb{S}^1 \times \Omega_0) \setminus 0$ . The kernel  $K_1$  has the oscillatory representation

$$K_1(z, t, e^{i\varphi}, z_1) = \int_{\mathbb{R}} e^{i\tau(t - 2 \operatorname{Re}(e^{i\varphi} z_1))} \frac{e^{i\varphi}(i\tau)}{\pi(z - z_1)} d\tau, \tag{5-5}$$

interpreted in the sense of distributions. The amplitude in (5-5) belongs to the standard space of symbols  $S_{1,0}^1$  on  $(\Omega_1 \times \mathbb{R} \times \mathbb{S}^1 \times \Omega_0) \times (\mathbb{R} \setminus 0)$  [Hörmander 1971]. Thus, using from that paper his notation and orders for Fourier integral (Lagrangian) distribution classes,  $K_1$  is of order  $1 + \frac{1}{2} - \frac{0}{4}$ , i.e.,  $K_1 \in I^0(\Lambda)$ . We conclude that  $T_1$  is an FIO of order 0 associated with the canonical relation

$$C \subset (T^*(\Omega_1 \times \mathbb{R} \times \mathbb{S}^1) \setminus 0) \times (T^*\Omega_0 \setminus 0), \tag{5-6}$$

written  $T_1 \in I^0(C)$ , where

$$C = \Lambda' := \{(z, t, e^{i\varphi}, \zeta, \tau, \Phi; z_1, \zeta_1) : (z, t, e^{i\varphi}, z_1; \zeta, \tau, \Phi, -\zeta_1) \in \Lambda\}. \tag{5-7}$$

The wave front set of  $K_1$  satisfies  $\operatorname{WF}(K_1) \subset \Lambda$  (and actually, by the particular form of  $K_1$ , equality holds). Hence, by the Hörmander–Sato lemma [Hörmander 1971, Theorem 2.5.14],  $\operatorname{WF}(T_1\mu) \subset C_0 \circ \operatorname{WF}(\mu)$ , with  $C$  considered as a set-theoretic relation from  $T^*\Omega_0 \setminus 0$  to  $T^*(\Omega_1 \times \mathbb{R} \times \mathbb{S}^1) \setminus 0$ .

We next consider the geometry of  $C$ , parametrized as

$$C = \{(z, 2\operatorname{Re}(e^{i\varphi} z_1), e^{i\varphi}, 0, \tau, 2\tau \operatorname{Im}(e^{i\varphi} z_1); z_1, 2\tau e^{-i\varphi}) : z \in \Omega_1, z_1 \in \Omega_0, e^{i\varphi} \in \mathbb{S}^1, \tau \in \mathbb{R} \setminus \{0\}\}. \quad (5-8)$$

$C$  is of dimension 6, while the natural projections to the left and right,  $\pi_L : C \rightarrow T^*(\Omega_1 \times \mathbb{R} \times \mathbb{S}^1) \setminus 0$  and  $\pi_R : C \rightarrow T^*\Omega_0 \setminus 0$ , are into spaces of dimensions 8 and 4, respectively.  $C$  satisfies the Bolker condition [Guillemin 1985; Guillemin and Sternberg 1977]:  $\pi_L$  is an immersion (which is equivalent to  $\pi_R$  being a submersion) and is globally injective.

However,  $C$  in fact satisfies a much stronger condition than the Bolker condition: the geometry of  $C$  is *independent* of  $z \in \Omega_1$ , and it is a canonical graph in the remaining variables. If for any  $z_0 \in \Omega_1$  we set  $K_1^{z_0} = K_1|_{z=z_0}$ , then one can factor  $C = 0_{T^*\Omega_1} \times C_0$  (with the obvious reordering of the variables), where  $0_{T^*\Omega_1}$  is the zero-section of  $T^*\Omega_1$  and

$$\begin{aligned} C_0 &:= \operatorname{WF}(K_1^{z_0})' = \{(2\operatorname{Re}(e^{i\varphi} z_1), e^{i\varphi}, \tau, 2\tau \operatorname{Im}(e^{i\varphi} z_1); z_1, 2\tau e^{-i\varphi}) : z_1 \in \Omega_0, e^{i\varphi} \in \mathbb{S}^1, \tau \in \mathbb{R} \setminus \{0\}\} \\ &\subset (T^*(\mathbb{R} \times \mathbb{S}^1) \setminus 0) \times (T^*\Omega_0 \setminus 0). \end{aligned} \quad (5-9)$$

(Note that  $C_0 = N^*L'_0$ , where

$$L_0 = \{(t, e^{i\varphi}, z_1) \in \mathbb{R} \times \mathbb{S}^1 \times \mathbb{C} : t - 2\operatorname{Re}(e^{i\varphi} z_1) = 0\}.)$$

From (5-8), (5-9) one can see that  $C$  satisfies the Bolker condition, but its product structure is in fact much more stringent.

Hence, it is reasonable to form determined (i.e., two-dimensional) data sets from two-dimensional slices of the full  $T_1$  by fixing  $z = z_0$ ; for these to correspond to boundary measurements, assume that  $z_0 \in \partial\Omega \subset \Omega_1$ . Thus, define  $T_1^{z_0} : \mathcal{E}'(\Omega_0) \rightarrow \mathcal{D}'(\mathbb{R} \times \mathbb{S}^1)$  by  $\mu(z_1) \rightarrow (T_1^{z_0}\mu)(t, \varphi) := \hat{w}_0(z_0, t, \varphi)$ .  $T_1^{z_0}$  has Schwartz kernel  $K_1^{z_0}$  given by (5-5), but with  $z$  fixed at  $z = z_0$ , and thus  $T_1^{z_0}$  is an FIO of order  $1 + \frac{1}{2} - \frac{4}{4} = \frac{1}{2}$  with canonical relation  $C_0$ , i.e.,  $T_1^{z_0} \in I^{\frac{1}{2}}(C_0)$ . Further, one easily checks from (5-9) that  $\pi_R : C_0 \rightarrow T^*\Omega_0 \setminus 0$  and  $\pi_L : C_0 \rightarrow T^*(\mathbb{R} \times \mathbb{S}^1) \setminus 0$  are local diffeomorphisms, injective if we either restrict  $\tau > 0$  or  $\phi \in [0, \pi)$ , in which case  $C_0$  becomes a global canonical graph.

Composing  $T_1^{z_0}$  with the backprojection operator  $(T_1^{z_0})^*$  then yields, by the transverse intersection calculus for FIOs [Hörmander 1971], a normal operator  $(T_1^{z_0})^*T_1^{z_0}$  which is a  $\Psi$ DO of order 1 on  $\Omega_0$ , i.e.,  $(T_1^{z_0})^*T_1^{z_0} \in \Psi^1(\Omega_0)$ . We will show that the normal operator is elliptic and thus admits a left parametrix,  $Q(z, D) \in \Psi^{-1}(\mathbb{C})$ , so that

$$Q(T_1^{z_0})^*T_1^{z_0} - I \text{ is a smoothing operator on } \mathcal{E}'(\Omega_0). \quad (5-10)$$

Therefore,  $T_1^{z_0}\mu$  determines  $\mu \bmod C^\infty$ , making it possible to determine the singularities of the Beltrami multiplier  $\mu$ , and hence those of the conductivity  $\sigma$ , from the singularities of  $T_1^{z_0}\mu$ . All of this follows from standard arguments once one shows that  $T_1^{z_0}$  is an elliptic FIO.

To establish this ellipticity, we may, because  $z_0 - z_1 \neq 0$  for  $z_1 \in \Omega_0$ , calculate the principal symbol  $\sigma_{\text{prin}}(T_1^{z_0})$  using (5-3). At a point of  $C_0$ , as given by the parametrization (5-9), we may calculate the

induced symplectic form  $\kappa_{C_0}$  on  $C_0$ ,

$$\kappa_{C_0} := \pi_R^*(\kappa_{T^*\Omega_0}) = -2\tau d\varphi \wedge (s(\varphi)dx' + c(\varphi)dy') + 2d\tau \wedge (c(\varphi)dx' - s(\varphi)dy'), \tag{5-11}$$

so that  $\kappa_{C_0} \wedge \kappa_{C_0} = 4\tau d\varphi \wedge d\tau \wedge dx' \wedge dy'$ , and the half density satisfies

$$|\kappa_{C_0} \wedge \kappa_C|^{1/2} = 2|\tau|^{1/2} |d\varphi \wedge d\tau \wedge dx' \wedge dy|^{1/2}.$$

From this it follows that

$$\sigma_{\text{prin}}(T_1^{z_0}) = \frac{-2e^{i\varphi}(i\tau)}{2|\tau|^{1/2}(z_0 - z_1)} = \frac{(-ie^{i\varphi}) \operatorname{sgn}(\tau)|\tau|^{1/2}}{z_0 - z_1},$$

which is elliptic of order  $\frac{1}{2}$  on  $C_0$ .

**Example.** Although (5-10) allows imaging of general  $\mu \in \mathcal{E}'(\Omega_0)$  from  $\omega_1(z_0, \cdot, \cdot)$ , consider the particular case where  $\mu$  is a piecewise smooth function with jumps across an embedded smooth curve  $\gamma = \{z : g(z) = 0\} \subset \Omega_0$  (not necessarily closed or connected), with unit normal  $n$ . In fact, consider the somewhat more general case of a  $\mu$  which is *conormal of order*  $m \in \mathbb{R}$ ,  $m \leq -1$ , with respect to  $\gamma$ , i.e., is of the form

$$\mu(z) = \int_{\mathbb{R}} e^{ig(z)\theta} a_m(x, \theta) d\theta, \tag{5-12}$$

where  $a_m$  belongs to the standard symbol class  $S_{1,0}^m(\Omega_0 \times (\mathbb{R} \setminus 0))$ . (In general, we will denote the orders or biorders of symbols by subscripts.) A  $\mu$  which is a piecewise smooth function with jumps across  $\gamma$  is of this form for  $m = -1$ ; for  $-2 < m < -1$ , a  $\mu$  given by (5-12) is piecewise smooth, as well as Hölder continuous of order  $-m - 1$  across  $\gamma$ . (Recall that uniqueness in the Calderón problem for  $C^\omega$  piecewise smooth conductivities was treated in [Kohn and Vogelius 1985] and some cases of conormal conductivities in [Greenleaf et al. 2003; Kim 2008].) As a Fourier integral distribution,  $\mu \in I^m(\Gamma)$  for the Lagrangian manifold

$$\Gamma := N^*\gamma = \{(z_1, \theta n(z_1)) : z_1 \in \gamma, \theta \in \mathbb{R} \setminus 0\} \subset T^*\Omega_0 \setminus 0. \tag{5-13}$$

By the transverse intersection calculus,  $T_1^{z_0}\mu \in I^{m+1/2}(\tilde{\Gamma})$ , where

$$\tilde{\Gamma} := C \circ \Gamma = \{(2 \operatorname{Re}(e^{i\varphi} z_1), e^{i\varphi}, \tau, 2\tau \operatorname{Im}(e^{i\varphi} z_1)) : z_1 \in \gamma, e^{i\varphi} = \overline{n(z_1)}, \tau \in \mathbb{R} \setminus 0\} \subset T^*(\mathbb{R} \times \mathbb{S}^1) \setminus 0. \tag{5-14}$$

Thus, for  $\varphi$  fixed,  $T_1^{z_0}\mu$  has singularities at those values of  $t$  of the form  $t = 2 \operatorname{Re}(e^{i\varphi} z_1)$  with  $z_1$  ranging over the points of  $\gamma$  with  $n(z_1) = e^{-i\varphi}$ . (Under a finite order of tangency condition on  $\gamma$ , for each  $\varphi$  there are only a finite number of such points.) These values of  $t$  depend on  $\varphi$  but *are independent of*  $z_0 \in \partial\Omega$ ; this reflects the complex principal-type geometry underlying the problem, which has propagated the singularities of  $\mu$  out to *all* of the boundary points of  $\Omega$ . Denoting these values of  $t$  by  $t_j(e^{i\varphi})$ , the distribution  $T_1^{z_0}\mu$  has Lagrangian singularities conormal of order  $m + \frac{1}{2}$  on  $\mathbb{R}$  at  $\{t_j\}$ , and thus is of magnitude  $\sim |t - t_j|^{-m-3/2}$  for  $-\frac{3}{2} < m \leq -1$ . In particular, if  $\mu$  is piecewise smooth with jumps, for which  $m = -1$ , the singularities have magnitude  $\sim |t - t_j|^{-1/2}$ .

**Remark.** More generally, since  $T_1^{z_0}$  is an elliptic FIO of order  $\frac{1}{2}$  associated to a canonical graph, if we denote the  $L^2$ -based Sobolev space of order  $s \in \mathbb{R}$  by  $H^s$ , it follows that if  $\mu \in H^s \setminus H^{s-1}$ , then  $T_1^{z_0} \mu \in H^{s-1/2} \setminus H^{s-3/2}$ , allowing us to image general singularities of  $\mu$  and hence  $\sigma$ .

**5B. “Averages” of  $\hat{\omega}_1$  and artifact removal.** As described above, each  $T_1^{z_0}$  is in  $I^{1/2}(C_0)$ ; the symbol depends on  $z_0$ , the canonical relation (5-9) does not, and we now take advantage of this. For any  $\mathbb{C}$ -valued weight  $a(\cdot)$  on  $\partial\Omega$ , define

$$\hat{\omega}_1^a(t, e^{i\varphi}) := \int_{\partial\Omega} \hat{\omega}_1(z_0, t, e^{i\varphi}) a(z_0) dz_0, \tag{5-15}$$

and denote by  $T_1^a$  the operator taking  $\mu(z_1) \rightarrow \hat{\omega}_1^a(t, e^{i\varphi})$ . (It will be clear from context when the superscript is a point  $z_0 \in \partial\Omega$  and when it is a function  $a(\cdot)$  on the boundary.) (We emphasize that (5-15) is a complex line integral.) Then  $T_1^a$  has kernel

$$\begin{aligned} K_1^a(t, e^{i\varphi}, z_1) &:= -2e^{i\varphi} \left[ \int_{\partial\Omega} \frac{a(z_0) dz_0}{z_0 - z_1} \right] \delta'(t - 2 \operatorname{Re}(e^{i\varphi} z_1)) \\ &= -4\pi i e^{i\varphi} \alpha(z_1) \delta'(t - 2 \operatorname{Re}(e^{i\varphi} z_1)), \end{aligned} \tag{5-16}$$

where

$$\alpha(z_1) = \frac{1}{2\pi i} \int_{\partial\Omega} \frac{a(z_0) dz_0}{z_0 - z_1}, \quad z_1 \in \Omega,$$

is the Cauchy (line) integral of  $a$ . We thus have

$$\sigma_{\text{prin}}(T_1^a) = 2\pi e^{i\varphi} \alpha(z_1) \operatorname{sgn}(\tau) |\tau|^{1/2} \quad \text{on } C_0,$$

and therefore  $(T_1^a)^* T_1^a \in \Psi^1(\Omega_0)$ , with

$$\sigma_{\text{prin}}((T_1^a)^* T_1^a)(z, \zeta) = 2\pi^2 |\alpha(z)|^2 |\zeta|,$$

since, by (5-9),  $|\tau| = \frac{1}{2} |\zeta'|$  on  $C_0$ . Thus,

$$(T_1^a)^* T_1^a = 2\pi^2 |\alpha|^2 \cdot |D_z| \text{ mod } \Psi^0(\Omega_0).$$

By choosing  $a \equiv (\pi\sqrt{2})^{-1}$  in (5-15), one has  $\alpha \equiv (\pi\sqrt{2})^{-1}$  on  $\Omega$  and  $\sigma_{\text{prin}}((T_1^a)^* T_1^a)(z, \zeta) = |\zeta|$ , yielding

$$(T_1^a)^* T_1^a = |D_z| \text{ mod } \Psi^0, \tag{5-17}$$

which faithfully reproduces the locations of the singularities of  $\mu$  and accentuates their strength by one derivative. This is, in the context of our reconstruction method, an analogue of local (or  $\Lambda$ -) tomography [Faridani et al. 1992].

Alternatively (now with the choice of  $a = 1/\pi$ ), one may obtain an exact *weighted, filtered back-projection* inversion formula,

$$(T_1^a)^* (|D_t|^{-1}) T_1^a = I \quad \text{on } L^2(\Omega_0). \tag{5-18}$$

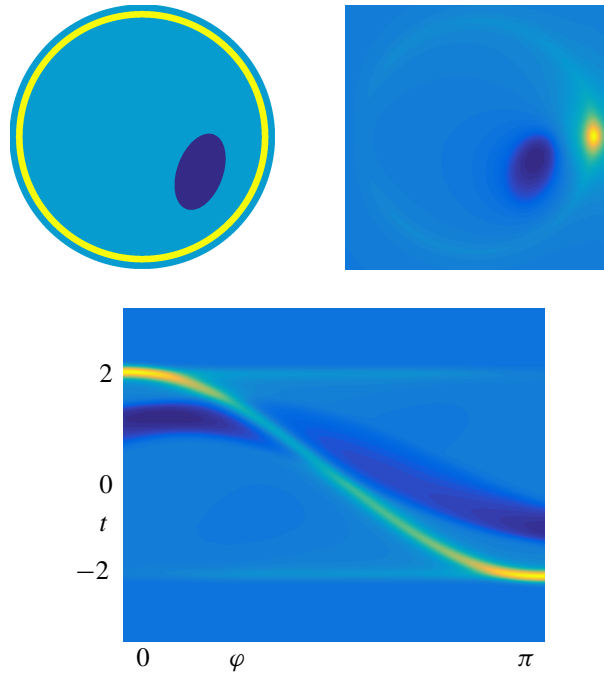


**Figure 4.** Artifacts from a single  $T_1^{z_0}$ . Top left: Phantom modeling hemorrhage (high conductivity inclusion) within skull (low conductivity shell). Bottom:  $T_1^{z_0} \mu$  for  $z_0 = 1$ . Top right: backprojection applied to  $T_1^{z_0} \mu$ .

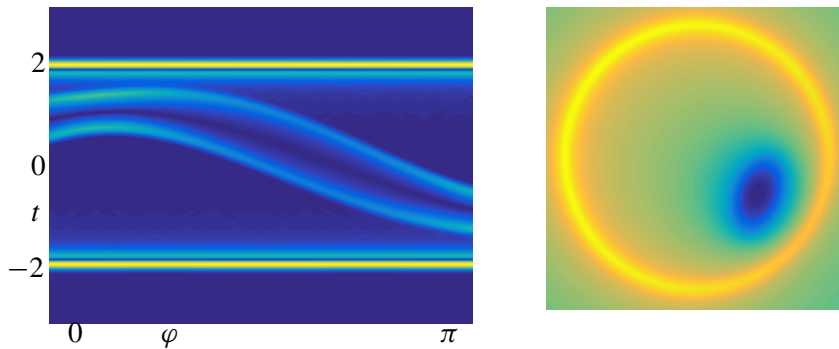


**Figure 5.** Artifact removal using weighted  $T_1^a$ . Left:  $T_1^a \mu$  for phantom in Figure 4. Right: reconstruction from  $T_1^a \mu$  using formula (5-18).

On the level of the principal symbol, this follows from the microlocal analysis above, again since  $|\tau| = \frac{1}{2}|\zeta'|$  on  $C_0$ ; for the exact result, note that

$$T_1^a = -\left(\frac{i\pi}{\sqrt{2}}\right)e^{i\varphi}\left(\frac{\partial}{\partial s}R\mu\right)\left(\frac{t}{2}, e^{i\varphi}\right), \tag{5-19}$$

where  $R$  is the standard Radon transform on  $\mathbb{R}^2$ ,

$$(Rf)(s, \omega) = \int_{x \cdot \omega = s} f(x) d^1x, \quad (s, \omega) \in \mathbb{R} \times S^1.$$

**Remark.** Note that if we take  $\Omega = \mathbb{D}$ , so that  $\partial\Omega$  can be parametrized by  $z_0 = e^{i\theta}$ , then (5-15) becomes

$$\hat{\omega}_1^a(t, e^{i\varphi}) = \int_0^{2\pi} \hat{\omega}_1(e^{i\theta}, t, e^{i\varphi}) i e^{i\theta} d\theta.$$

Thus, the weight is (slowly) oscillatory when expressed in terms of  $d\theta$ , but through destructive interference suppresses the artifacts present in each individual  $\hat{\omega}_1^{z_0}$ . Figure 5 illustrates, with a skull/hemorrhage phantom how using this simple weight removes the artifacts caused by the rapid change in the amplitude and phase of the Cauchy factor  $(z_0 - z_1)^{-1}$ , shown in Figure 4.

### 6. Analysis of $\hat{\omega}_2$

Just as the introduction of polar coordinates and partial Fourier transform, applied to the zeroth-order term in the Neumann expansion (i.e., the Fréchet derivative of the scattering map at  $\mu = 0$ ), give rise to a term linear in  $\mu$ , their application to the first-order term (4-10) gives rise to a term which is bilinear in  $\mu$ . Wave front set analysis shows that this nonlinearity gives rise to two distinct types of singularities; we will see in Section 10 that both of these are visible in the numerics, and need to be taken into account to give good reconstruction based on  $\hat{\omega}_1^a$ .

We can rewrite (4-10) as

$$\omega_2(z, k) = P(\alpha(\bar{P}\bar{\alpha})) + P(v(\bar{S}\bar{\alpha})),$$

where the linear operators  $\bar{P}, \bar{S}$  are defined by  $\bar{P}(f) = \overline{P(\bar{f})}$  and  $\bar{S}(f) = \overline{S(\bar{f})}$ . The kernels of  $\bar{P}, \bar{S}$  are just the complex conjugates of the kernels of  $P, S$  in (3-11), (3-12), respectively. We now denote the two interior variables in  $\Omega_0$  by  $z_1$  and  $z_2$ ; using (3-9), one sees that

$$\begin{aligned} \omega_2(z, k) = & \frac{-k^2}{\pi^2} \int_{\mathbb{C}} \int_{\mathbb{C}} \frac{e^{-2i \operatorname{Re}(kz_1)} \mu(z_1)}{z_1 - z} \frac{e^{2i \operatorname{Re}(kz_2)} \mu(z_2)}{\bar{z}_2 - \bar{z}_1} d^2z_1 d^2z_2 \\ & + \frac{ik}{\pi^2} \int_{\mathbb{C}} \int_{\mathbb{C}} \frac{e^{-2i \operatorname{Re}(kz_1)} \mu(z_1)}{z_1 - z} \frac{e^{2i \operatorname{Re}(kz_2)} \mu(z_2)}{(\bar{z}_2 - \bar{z}_1)^2} d^2z_1 d^2z_2. \end{aligned} \quad (6-1)$$

Thus, for  $z_0 \in \partial\Omega$ ,

$$\hat{\omega}_2(z_0, t, e^{i\varphi}) = \int_{\mathbb{R}} e^{-it\tau} \omega_1(z_0, \tau e^{i\varphi}) d\tau = \int_{\mathbb{C}} \int_{\mathbb{C}} K_1(z_0, t, e^{i\varphi}; z_1, z_2) \mu(z_1) \mu(z_2) d^2z_1 d^2z_2 \quad (6-2)$$

is given by a bilinear operator acting on  $\mu \otimes \mu$ , with kernel

$$K_2^{z_0}(t, e^{i\varphi}; z_1, z_2) = \frac{1}{\pi^2} \left( \frac{e^{2i\varphi} \delta''(t + 2 \operatorname{Re}(e^{i\varphi}(z_1 - z_2)))}{(z_1 - z_0)(\bar{z}_2 - \bar{z}_1)} + \frac{e^{i\varphi} \delta'(t + 2 \operatorname{Re}(e^{i\varphi}(z_1 - z_2)))}{(z_1 - z_0)(\bar{z}_2 - \bar{z}_1)^2} \right). \quad (6-3)$$

$K_2^{z_0}$  has multiple singularities, but, as in the case of  $K_1$ , the fact that  $|z_1 - z_0| \geq c > 0$  for  $z_0 \in \partial\Omega$  and  $z_1 \in \operatorname{supp}(\mu) \subset \Omega_0$  eliminates the singularities at  $\{z_1 - z_0 = 0\}$ . The remaining singularities put  $K_2^{z_0}$  in

the general class of paired Lagrangian distributions introduced in [Melrose and Uhlmann 1979; Guillemin and Uhlmann 1981]. In fact,  $K_2^{z_0}$  lies in a more restrictive class of *nested conormal distributions*, see [Greenleaf and Uhlmann 1990], associated with the pair (independent of  $z_0$ )

$$L_1 := \{t + 2 \operatorname{Re}(e^{i\varphi}(z_1 - z_2)) = 0\} \supset L_3 := \{t + 2 \operatorname{Re}(e^{i\varphi}(z_1 - z_2)) = 0, z_1 - z_2 = 0\} = \{t = 0, z_2 = z_1\}. \quad (6-4)$$

(The subscripts are chosen to indicate the respective codimensions in  $\mathbb{R}_t \times \mathbb{S}_\varphi^1 \times \Omega_{0, z_1} \times \Omega_{0, z_2}$ .) These submanifolds have conormal bundles,

$$\Lambda_1 := N^*L_1, \quad \Lambda_3 := N^*L_3 \subset T^*(\mathbb{R}_t \times \mathbb{S}_\varphi^1 \times \Omega_{0, z_1} \times \Omega_{0, z_2}) \setminus 0,$$

and  $\operatorname{WF}(K_2^{z_0}) \subseteq \Lambda_1 \cup \Lambda_3$ . (As with  $K_1^{z_0}$ , one can show from (6-3) that equality holds.)

**6A. Bilinear wave front set analysis.** Define  $\hat{\omega}_2^{z_0} = \hat{\omega}_2|_{z=z_0}$ . Since  $\hat{\omega}_2^{z_0}(t, e^{i\varphi}) = \langle K_2^{z_0}(t, e^{i\varphi}, \cdot, \cdot), \mu \otimes \mu \rangle$ , we have

$$\operatorname{WF}(\hat{\omega}_2^{z_0}) \subset \operatorname{WF}(K_2^{z_0})' \circ \operatorname{WF}(\mu \otimes \mu) \subset (\Lambda_1' \cup \Lambda_3') \circ \operatorname{WF}(\mu \otimes \mu).$$

Parametrizing  $\Lambda_1, \Lambda_3$  in the usual way as conormal bundles, multiplying the variables dual to  $z_1, z_2$  by  $-1$  and then separating the variables on the left and right, we obtain canonical relations in  $T^*(\mathbb{R} \times \mathbb{S}^1) \times T^*(\Omega_0 \times \Omega_0)$ ,

$$C_1 := \Lambda_1' = \{(-2 \operatorname{Re}(e^{i\varphi}(z_1 - z_2)), e^{i\varphi}, \tau, -2\tau \operatorname{Im}(e^{i\varphi}(z_1 - z_2)); z_1, z_2, -2\tau e^{i\varphi}, 2\tau e^{i\varphi}) \\ : e^{i\varphi} \in \mathbb{S}^1, z_1, z_2 \in \Omega_0, \tau \in \mathbb{R} \setminus 0\}, \quad (6-5)$$

$$C_3 := \Lambda_3' = \{(0, e^{i\varphi}, \tau, 0; z_1, z_1, \zeta, -\zeta) : e^{i\varphi} \in \mathbb{S}^1, z_1 \in \Omega_0, (\tau, \zeta) \in \mathbb{R}^3 \setminus 0\}. \quad (6-6)$$

Representing  $\mu \otimes \mu = \mu(z_1)\mu(z_2)$  as  $(\mu \otimes 1) \cdot (1 \otimes \mu)$ , from a basic result concerning wave front sets of products [Hörmander 1971, Theorem 2.5.10], one sees that

$$\begin{aligned} \operatorname{WF}(\mu \otimes \mu) &\subseteq \operatorname{WF}(\mu \otimes 1) \cup \operatorname{WF}(1 \otimes \mu) \cup (\operatorname{WF}(\mu \otimes 1) + \operatorname{WF}(1 \otimes \mu)) \\ &\subseteq (\operatorname{WF}(\mu) \times \mathcal{O}_{T^*\Omega_0}) \cup (\mathcal{O}_{T^*\Omega_0} \times \operatorname{WF}(\mu)) \cup (\operatorname{WF}(\mu) \times \operatorname{WF}(\mu)), \end{aligned} \quad (6-7)$$

where the sets are interpreted as subsets of  $T^*\mathbb{C}^2 \setminus 0$ , writing elements as either  $(z_1, z_2; \zeta_1, \zeta_2)$  or  $(z_1, \zeta_1; z_2, \zeta_2)$ .

Since  $\zeta_1 \neq 0, \zeta_2 \neq 0$  at all points of  $C_1$ , and  $\zeta_1 = 0 \iff \zeta_2 = 0$  on  $C_3$ , the relation  $C_1 \cup C_3$ , when applied to the first two terms on the right-hand side of (6-7), gives the empty set.

On the other hand,  $C_1 \cup C_3$ , when applied to  $\operatorname{WF}(\mu) \times \operatorname{WF}(\mu)$ , contributes nontrivially to  $\operatorname{WF}(\hat{\omega}_2^{z_0})$ . First, the application of  $C_3$  gives

$$\{(0, e^{i\varphi}, \tau, 0) : \exists z_1 \text{ such that } (z_1, \tau e^{-i\varphi}) \in \operatorname{WF}(\mu)\} \subset N^*\{t = 0\}. \quad (6-8)$$

Secondly,  $C_1$  yields a contribution to  $\operatorname{WF}(\hat{\omega}_2^{z_0})$  contained in what we call the CGO *two-scattering* of  $\mu$ , defined by

$$\begin{aligned} \operatorname{Sc}^{(2)}(\mu) &:= \{(-2 \operatorname{Re}(e^{i\varphi}(z_1 - z_2)), e^{i\varphi}, \tau, -2\tau \operatorname{Im}(e^{i\varphi}(z_1 - z_2))) \\ &\quad : \exists z_1, z_2 \in \Omega_0 \text{ such that } (z_1, \tau e^{-i\varphi}), (z_2, -\tau e^{-i\varphi}) \in \operatorname{WF}(\mu)\}. \end{aligned} \quad (6-9)$$

Thus, pairs of points in  $\text{WF}(\mu)$  with spatial coordinates  $z_1, z_2$  and antipodal covectors  $\pm\tau e^{-i\varphi}$  give rise to elements of  $\text{WF}(\hat{\omega}_2^{z_0})$  at  $t = -2 \text{Re}(e^{i\varphi}(z_1 - z_2))$ . Note that the expression in (6-8) is not necessarily contained in  $\text{Sc}^{(2)}(\mu)$ , even if we allow  $z_1 = z_2$  in (6-9), since  $\text{WF}(\mu)$  is not necessarily symmetric under  $(z, \zeta) \rightarrow (z, -\zeta)$  (although this does hold for  $\mu$  which are smooth with jumps).

For later use, it is also convenient to define

$$\text{Sc}^{(0)}(\mu) := N^*\{(t, e^{i\varphi}) : t = 0\} \quad \text{and} \quad \text{Sc}^{(1)}(\mu) := C_0 \circ \text{WF}(\mu), \tag{6-10}$$

where  $C_0$  is as in (5-9) above, so that the wave front set analysis so far can be summarized as

$$\text{WF}(\hat{\omega}_1) \subset \text{Sc}^{(1)}(\mu) \quad \text{and} \quad \text{WF}(\hat{\omega}_2) \subset \text{Sc}^{(0)}(\mu) \cup \text{Sc}^{(2)}(\mu). \tag{6-11}$$

This is extended to general  $\text{WF}(\hat{\omega}_n)$  in (7-6) below.

**Remarks.** (1) Note that if the  $\hat{\omega}_2^{z_0}$  are averaged out using a function  $a(z_0)$  on  $\partial\Omega$  as was done for  $\hat{\omega}_1$ , the wave front analysis above is still valid for the resulting  $\hat{\omega}_2^g$ , and we will refer to either as simply  $\hat{\omega}_2$  in the following discussion.

(2) It follows from (6-8) that for any  $\mu$  with  $\mu \notin C^\infty$ , and any  $z_0 \in \partial\Omega$ , we always will see singularities of  $\hat{\omega}_2$  at  $t = 0$ . The only dependence on  $\mu$  of these artifacts in  $\text{WF}(\hat{\omega}_2)$  is determined by the incident directions  $\varphi$  of the complex plane wave for which they occur, as dictated by (6-8).

(3) In addition, by (6-9), any spatially separated singularities of  $\mu$  with antipodal covectors  $\pm\zeta = \pm(\xi, \eta)$  give rise to singularities of  $\hat{\omega}_2$  at  $t = -2 \text{Re}(e^{i\varphi}(z_1 - z_2))$ ,  $\varphi = -\arg(\zeta)$ . Under translations, neither the covectors nor the differences  $z_1 - z_2$  associated to such scatterings change, although the factor  $(z_1 - z)^{-1}$  in the kernel (6-3), which is evaluated at  $z = z_0$ , does. Hence, the locations and orders of these artifacts (but not their magnitude or phase) are essentially independent of translations within  $\Omega_0$  of inclusions present in  $\mu$ .

Given the invertibility of  $T_1^a \text{ mod } C^\infty$  (at least for constant weight  $a(\cdot)$ ), from the point of view of our reconstruction method, the singularities of  $\hat{\omega}_2^a$  at  $t = 0$  and at  $\text{Sc}^{(2)}(\mu)$ , although part of  $\hat{\omega}$ , produce artifacts which interfere with reconstruction of the singularities of  $\mu$  and should either be better characterized or filtered out. In the next subsection, we do the former for a class of  $\mu$  which includes those which are piecewise smooth with jumps.

**6B. Bilinear operator theory.** Not only is  $\text{WF}(K_2^{z_0}) \subset \Lambda_1 \cup \Lambda_3$ , but in fact  $K_1^{z_0}$  belongs to the class of nested conormal distributions associated with the pair  $L_1 \supset L_3$ , see [Greenleaf and Uhlmann 1990], and thus to the Lagrangian distributions associated with the cleanly intersecting pair  $\Lambda_1, \Lambda_3$ ,

$$K_2^{z_0} \in I^{1,0}(\Lambda_1, \Lambda_3) + I^{1,-1}(\Lambda_1, \Lambda_3).$$

Any  $K_2^a$  is a linear superposition of these and thus belongs to the same class. The linear operators  $T_2^{z_0}, T_2^a : \mathcal{E}'(\Omega_0 \times \Omega_0) \rightarrow \mathcal{D}'(\mathbb{R} \times \mathbb{S}^1)$  with Schwartz kernels  $K_2^{z_0}, K_2^a$  respectively, which we will refer to simply as  $T_2$ , thus belong to a sum of spaces of singular Fourier integral operators,  $I^{1,0}(C_1, C_3) + I^{1,-1}(C_1, C_3)$ , and have some similarity to singular Radon transforms [Phong and Stein 1986], see also [Greenleaf and

Uhlmann 1990], but (i) this underlying geometry has to our knowledge not been studied before; and (ii) we are interested in *bilinear* operators with these kernels. Rather than pursuing optimal bounds for  $T_2$  on function spaces, we shall focus on the goal of characterizing the singularities of  $\hat{\omega}_2$  when  $\mu$  is piecewise smooth with jumps. We will show that, away from  $t = 0$ ,  $\hat{\omega}_2$  is half a derivative smoother than  $\hat{\omega}_1$ . On the other hand, at  $t = 0$  it is possible for  $\hat{\omega}_2$  to be as singular as the strongest singularities of  $\hat{\omega}_1$ ; this is present in the full  $\hat{\omega}$  (computed from the DN data) and produces strong artifacts, which can be seen in numerics when attempting to reconstruct  $\mu$ . For this reason, data should be either preprocessed by filtering out a neighborhood of  $t = 0$  before applying backprojection, or alternatively one should resort to the subtraction techniques discussed in Section 8.

It will be helpful to work (as with the example (5-12) above) in the slightly greater generality of distributions (still denoted by  $\mu$ ) that are conormal for a curve  $\gamma \subset \Omega_0$ , having an oscillatory integral representation such as (5-12) with an amplitude of some order  $m \in \mathbb{R}$ . For such a  $\mu$  (even for one not coming from a conductivity), we may still define both  $\hat{\omega}_1^{z_0}$  and  $\hat{\omega}_1^a$  (denoted generically by  $\hat{\omega}_1$ ), and they belong to  $I^{m+1/2}(\tilde{\Gamma})$ , where  $\tilde{\Gamma} = C_0 \circ N^*\gamma \subset T^*(\mathbb{R} \times \mathbb{S}^1) \setminus 0$  is as in (5-14). We also define  $\hat{\omega}_2 := T_2^{z_0}(\mu \otimes \mu)$  or  $T_2^a(\mu \otimes \mu)$ .

To make the microlocal analysis of  $\hat{\omega}_2$  tractable, we now impose a curvature condition on  $\gamma$ : since  $\nabla g(z) \perp T_z\gamma$  at a point  $z \in \gamma$ , we have  $i\nabla g(z) \in T_z g$ ; thus,  $\gamma$  has nonzero Gaussian curvature at  $z$  if and only if

$$(i\nabla g(z))^t \nabla^2 g(z) (i\nabla g(z)) \neq 0, \tag{6-12}$$

which we henceforth assume holds at all points of  $\gamma$  (or at least at all  $z \in \text{sing supp } \mu \subset \gamma$ , which is all that matters).

Note that (6-12) implies the finite-order tangency condition referred to in the Example of Section 5A, so that for each  $e^{i\varphi} \in \mathbb{S}^1$ , we have  $\hat{\omega}_0(\cdot, e^{i\varphi})$  is singular at a finite number of values  $t = t_j(e^{i\varphi})$ .

**Theorem 6.1.** *Under the curvature assumption (6-12),*

- (i)  $\text{Sc}^{(2)}(\mu)$ , defined as in (6-9), is a smooth Lagrangian manifold in  $T^*(\mathbb{R} \times \mathbb{S}^1) \setminus 0$ ; and
- (ii) if  $\mu$  is as in (5-12) for some  $m \in \mathbb{R}$ , then

$$\hat{\omega}_2 = T_2^{z_0}(\mu \otimes \mu) \in I^{2m+3/2, -1/2}(\text{Sc}^{(2)}(\mu), \text{Sc}^{(0)}(\mu)). \tag{6-13}$$

Microlocally away from  $\Lambda_0 \cap \Lambda_1$ , a distribution  $u \in I^{p,l}(\Lambda_0, \Lambda_1)$  belongs to  $I^p(\Lambda_1 \setminus \Lambda_0)$  and to  $I^{p+l}(\Lambda_0 \setminus \Lambda_1)$  [Melrose and Uhlmann 1979; Guillemin and Uhlmann 1981]. Thus,  $\hat{\omega}_2 \in I^{2m+1}(\text{Sc}^{(2)}(\mu))$  on  $\text{Res}^{(2)}(\mu) \setminus N^*\{t = 0\}$  and hence is smoother than  $\hat{\omega}_1 \in I^{m+1/2}(\tilde{\Gamma})$  if  $m < -\frac{1}{2}$ . In contrast, on  $N^*\{t = 0\} \setminus \text{Sc}^{(2)}(\mu)$ , one has  $\hat{\omega}_2 \in I^{2m+3/2}(N^*\{t = 0\})$ , which is guaranteed to be smoother than  $\hat{\omega}_1$  only if  $m < -1$ .

In particular, for  $m = -1$ , corresponding to  $\sigma$  (and hence  $\mu$ ) being piecewise smooth with jumps, one has  $\hat{\omega}_2 \in I^{-1}(\text{Sc}^{(2)}(\mu))$ , while  $\hat{\omega}_1 \in I^{-1/2}(\tilde{\Gamma})$ , so that these artifacts are half a derivative smoother than the faithful image of  $\mu$  encoded by  $\hat{\omega}_1$ . On the other hand, the singularity of  $\hat{\omega}_2$  at  $N^*\{t = 0\}$  can be just as strong as the singularity of  $\hat{\omega}_1$  at  $\tilde{\Gamma}$ .

To summarize: for conductivities with jumps, applying standard Radon transform backprojection methods to the full data  $\hat{w}$ , or even its approximation  $\hat{w}_1 + \hat{w}_2$ , rather than just  $\hat{w}_1$  (which is not measurable directly) can result in artifacts which are smoother than the leading singularities only if one filters out a neighborhood of  $t = 0$ .

To see (i) and (ii), start by noting from (6-3) that  $T_2(\mu \otimes \mu)(t, e^{i\varphi})$  is a sum of two terms of the form

$$\int e^{i\Phi} a_{p,l}(*; \tau; \sigma) b_m(z_1; \theta_1) b_m(z_2; \theta_2) d\theta_1 d\theta_2 dz_1 dz_2 d\sigma d\tau, \tag{6-14}$$

where (recalling that  $g$  is a defining function for  $\gamma$ ),

$$\begin{aligned} \Phi &= \Phi(t, e^{i\varphi}, z_1, z_2, \tau, \sigma, \theta_1, \theta_2) \\ &:= \tau(t + 2 \operatorname{Re}(e^{i\varphi}(z_1 - z_2))) + \sigma \cdot (z_1 - z_2) + \theta_1 g(z_1) + \theta_2 g(z_2), \end{aligned} \tag{6-15}$$

$b_m \in S_{1,0}^m(\Omega_0 \times (\mathbb{R} \setminus 0))$ , and the  $a_{p,l}$  are product-type symbols satisfying

$$|\partial_{t,\varphi,z_1,z_2}^\gamma \partial_\sigma^\beta \partial_\tau^\alpha a_{p,l}(*; \tau; \sigma)| \lesssim \langle \tau \rangle^{p-\alpha} \langle \sigma \rangle^{l-|\beta|}$$

on  $(\mathbb{R} \times \mathbb{S}^1 \times \Omega_0 \times \Omega_0) \times \mathbb{R}_\tau \times \mathbb{R}_\sigma^2$ , (the  $*$  denoting all of the spatial variables) of biorders  $(p, l) = (2, -1)$  and  $(1, 0)$ , respectively. As can be seen from (6-5), (6-6),

$$C_1, C_3 \subset \{\zeta_2 = -\zeta_1, |\zeta_1| = 2|\tau|\} \subset \{|\zeta_1| = |\zeta_2| = 2|\tau|\},$$

so one can microlocalize the amplitudes in (6-14) to  $\{|\theta_1| \sim |\theta_2| \sim |\tau|\}$  and thus replace the  $a_{p,l} \cdot b_m \cdot b_m$  by amplitudes

$$a_{p+2m,l}(*; (\tau, \theta_1, \theta_2); \sigma) \in S^{p+2m,l}(\mathbb{R} \times \mathbb{S}^1 \times \Omega_0 \times \Omega_0 \times (\mathbb{R}_{\tau,\theta_1,\theta_2}^3 \setminus 0) \times \mathbb{R}_\sigma^2)$$

with biorders  $(2m + 2, -1)$  and  $(2m + 1, 0)$ , respectively.

Now homogenize the variables  $z_1, z_2$ , by defining phase variables  $\eta_j := \tau z_j \quad j = 1, 2$ . In terms of the estimates for derivatives, the new phase variables are grouped with the elliptic variables  $(\tau, \theta_1, \theta_2)$ ; furthermore, the change of variables involves a Jacobian factor of  $\tau^{-4}$ , so that, mod  $C^\infty$ , (6-14) becomes

$$\int e^{i\tilde{\Phi}} a_{\tilde{p},\tilde{l}}(*; (\tau, \theta_1, \theta_2, \eta_1, \eta_2); \sigma) d\tau d\theta_1 d\theta_2 d\eta_1 d\eta_2 d\sigma, \tag{6-16}$$

with

$$\begin{aligned} \tilde{\Phi} &= \tilde{\Phi}(t, e^{i\varphi}; \tau, \theta_1, \theta_2, \eta_1, \eta_2; \sigma) \\ &:= \tau t + 2 \operatorname{Re}(e^{i\varphi}(\eta_1 - \eta_2)) + \theta_1 g\left(\frac{\eta_1}{\tau}\right) + \theta_2 g\left(\frac{\eta_2}{\tau}\right) + \sigma \cdot \left(\frac{\eta_1 - \eta_2}{\tau}\right) \end{aligned} \tag{6-17}$$

on  $(\mathbb{R} \times \mathbb{S}^1) \times (\mathbb{R}_{\tau,\theta_1,\theta_2,\eta_1,\eta_2}^7 \setminus 0) \times \mathbb{R}_\sigma^2$  and with amplitude biorders  $(\tilde{p}, \tilde{l}) = (2m - 2, -1)$  and  $(2m - 3, 0)$ , respectively. We interpret  $\tilde{\Phi}$  as (a slight variation of) a multiphase function in the sense of [Mendoza 1982]: one can check that  $\tilde{\Phi}_0 := \tilde{\Phi}|_{\sigma=0}$  is a nondegenerate phase function (i.e., clean with excess  $e_0 = 0$ ) which parametrizes  $\operatorname{Sc}^{(2)}(\mu)$  (which is thus a smooth Lagrangian). One does this by verifying, using (6-12), that  $d_{(t,\varphi,\tau,\theta_1,\theta_2,\eta_1,\eta_2),(\tau,\theta_1,\theta_2,\eta_1,\eta_2)}^2 \tilde{\Phi}_0$  has maximal rank at  $\{d_{(\tau,\theta_1,\theta_2,\eta_1,\eta_2)} \tilde{\Phi}_0 = 0\}$ , namely  $= 7$ . On the other hand, the full phase function  $\tilde{\Phi}$  parametrizes  $N^*\{t = 0\}$ , but rather than being nondegenerate,

it is clean with excess  $e_1 = 1$ , i.e.,  $d_{(t,\phi,\tau,\theta_1,\theta_2,\eta_1,\eta_2,\sigma),(\tau,\theta_1,\theta_2,\eta_1,\eta_2,\sigma)}^2 \tilde{\Phi}$  has constant rank  $9 - 1 = 8$  at  $\{d_{(\tau,\theta_1,\theta_2,\eta_1,\eta_2,\sigma)} \tilde{\Phi} = 0\}$ . (See [Hörmander 1985] for a discussion of clean phase functions.) A slight modification of the results in [Mendoza 1982] yields the following.

**Proposition 6.2.** *Suppose two smooth conic Lagrangians  $\Lambda_0, \Lambda_1 \subset T^*\mathbb{R}^n \setminus 0$  intersect cleanly in codimension  $k$ . Let  $\phi(x, \theta, \sigma)$  be a phase function on  $\mathbb{R}^n \times (\mathbb{R}^{N+M} \setminus 0)$  such that parametrizes  $\Lambda_1$  cleanly with excess  $e_1 \geq 0$  and  $\phi_0(x, \theta) := \phi|_{\sigma=0}$  parametrizes  $\Lambda_0$  cleanly with excess  $e_0 \geq 0$ . Suppose further that  $a \in S^{\tilde{p}, \tilde{l}}(\mathbb{R}^n \times (\mathbb{R}^N \setminus 0) \times \mathbb{R}^M)$ . Then,*

$$u(x) := \int_{\mathbb{R}^{N+M}} e^{i\phi_1(x,\theta,\sigma)} a(x, \theta, \sigma) d\theta d\sigma \in I^{p', l'}(\Lambda_0, \Lambda_1),$$

with

$$p' = \tilde{p} + \tilde{l} + \frac{N + M + e_0 + e_1}{2} - \frac{n}{4}, \quad l' = -\tilde{l} - \frac{M + e_1}{2}.$$

Applying the proposition to each of the two biorders  $(\tilde{p}, \tilde{l}) = (2m - 2, -1)$  and  $(2m - 3, 0)$  from above, we see that  $T_2^{z_0}(\mu \otimes \mu)$ , as given by the expression (6-16), is a sum of two terms,

$$\hat{\omega}_2^{z_0} = T_2^{z_0}(\mu \otimes \mu) \in (I^{2m+3/2, -1/2} + I^{2m+3/2, -3/2})(\text{Sc}^{(2)}(\mu), N^*\{t = 0\}).$$

Recalling that  $N^*\{t = 0\} = \text{Sc}^{(0)}(\mu)$  and also that  $I^{p', l''} \subset I^{p', l'}$  for  $l'' \leq l'$ , this yields (6-13), finishing the proof of Theorem 6.1. □

### 7. Higher-order terms

**7A. Multilinear wave front set analysis.** For  $n \geq 3$ , and for any conductivity  $\sigma$ , one can analyze  $\text{WF}(\hat{\omega}_n^{z_0})$  and  $\text{WF}(\hat{\omega}_n^a)$  by  $n$ -linear versions of the case  $n = 2$  treated in Section 6A, starting with the kernels. For  $\hat{\omega}_n^{z_0}$ , we denote these by  $K_n(t, e^{i\varphi}, z_1, \dots, z_n)$ ; i.e.,  $\hat{\omega}_n^{z_0}$  is given by

$$\begin{aligned} \hat{\omega}_n^{z_0}(t, e^{i\varphi}) &= T_n^{z_0}(\mu \otimes \dots \otimes \mu) \\ &:= \int_{\mathbb{C}^n} K_n^{z_0}(t, e^{i\varphi}; z_1, \dots, z_n) \mu(z_1) \dots \mu(z_{n+1}) d^2 z_1 \dots d^2 z_n. \end{aligned} \tag{7-1}$$

The kernel for  $\hat{\omega}_n^a$  has the same geometry and orders, but amplitudes  $a(\cdot)$ -averaged in  $z_0$ , which does not affect the following analysis.

$K_n^{z_0}$  is a sum of  $2^{n-1}$  terms of the form, for  $\vec{\epsilon} \in \{0, 1\}^{n-1}$ ,

$$c_{\vec{\epsilon}} \cdot \frac{\delta^{(n+1-|\vec{\epsilon}|)}(t + (-1)^{n+1} 2 \text{Re}(e^{i\varphi} \sum_{j=1}^n (-1)^j z_j))}{(z_0 - z_1)(\bar{z}_1 - \bar{z}_2)^{1+\epsilon_1} (\bar{z}_2 - \bar{z}_3)^{1+\epsilon_2} \dots (\bar{z}_{n-1} - \bar{z}_n)^{1+\epsilon_{n-1}}}, \tag{7-2}$$

each with total homogeneity  $-(2n + 1)$  in  $(t, z_0, \dots, z_n)$ . These have singularities all in the same locations, namely on a lattice of submanifolds of  $\mathbb{R} \times \mathbb{S}^1 \times \mathbb{C}^n$ . For each  $J \in \mathcal{J} = \{J : J \subset \{1, \dots, n - 1\}\}$ , as in (4-14), let

$$L_n^J := \left\{ t + (-1)^{n+1} 2 \text{Re} \left( e^{i\varphi} \sum_{j=1}^n (-1)^j z_j \right) = 0 : z_j - z_{j+1} = 0 \text{ for all } j \in J \right\}. \tag{7-3}$$

One has  $\text{codim}(L_n^J) = 1 + 2|J|$  and  $L_n^J \supset L_n^{J'}$  if and only if  $J \subset J'$ . Rather than using set notation, we sometimes simply list the elements of  $J$ . The unique maximal element of the lattice is the hypersurface

$$L_n^\emptyset := \left\{ t + (-1)^{n+1} 2 \operatorname{Re} \left( e^{i\varphi} \sum_{j=1}^n (-1)^j z_j \right) = 0 \right\},$$

while the unique minimal one is

$$L_n^{12\dots(n-1)} = \{t = 0, z_1 = z_2 = \dots = z_n\}.$$

(This notation replaces that used earlier for  $n = 1, 2$ : what was previously denoted by  $L_0$  is now  $L_1^\phi$ , and  $L_1 = L_2^\phi, L_3 = L_2^1$ .)

As stated above,

$$\operatorname{sing\,supp}(K_n^{z_0}) = \bigcup_{J \in \mathcal{J}} L_n^J$$

and, in fact,

$$\operatorname{WF}(K_n^{z_0}) = \bigcup_{J \in \mathcal{J}} N^* L_n^J, \tag{7-4}$$

with the fact that equality holds (rather than just the  $\subset$  containment) following from the nonvanishing in all directions at infinity of the Fourier transforms of  $\delta^{(m)}, \bar{z}^{-1}$  and  $\bar{z}^{-2}$ . (However, we only need the containment, not equality, in what follows.)

Define canonical relations

$$C_n^J := N^*(L_n^J)' \subset (T^*(\mathbb{R} \times \mathbb{S}^1) \times T^*\mathbb{C}^n) \setminus 0,$$

sometimes also denoting  $C_n^\emptyset$  simply by  $C_n$ . The linear operators  $T_n^{z_0} : \mathcal{E}'(\mathbb{C}^n) \rightarrow \mathcal{D}'(\mathbb{R} \times \mathbb{S}^1)$  with kernels  $K_n^{z_0}$  are (as  $n$  varies) interesting prototypes of generalized Fourier integral operators associated with the lattices  $\{C_n^J : J \in \mathcal{J}\}$  of canonical relations intersecting cleanly pairwise. There is to our knowledge no general theory of such operators, but in any case, we can describe the wave front relation as follows. Let  $\tilde{\Sigma}^m$  denote the alternating sum

$$\tilde{\Sigma}^m := z_1 - z_2 + \dots + (-1)^{m+1} z_m.$$

**Definition 7.1.** In  $T^*(\mathbb{R} \times \mathbb{S}^1) \setminus 0$ , define

$$\operatorname{Sc}^{(0)}(\mu) = \{(0, e^{i\varphi}, \tau, 0) : \exists z \in \Omega \text{ such that } (z, \tau e^{-i\varphi}) \in \operatorname{WF}(\mu)\} \subset N^*\{t = 0\},$$

and, for  $m \geq 1$ , let

$$\begin{aligned} \operatorname{Sc}^{(m)}(\mu) = & \left\{ \left( (-1)^{m+1} 2 \operatorname{Re}(e^{i\varphi} \tilde{\Sigma}^m), e^{i\varphi}, \tau, (-1)^m 2\tau \operatorname{Im}(e^{i\varphi} \tilde{\Sigma}^m) \right) \right. \\ & \left. : \exists z_1, \dots, z_m \text{ such that } (z_j, (-1)^{j+1} \tau e^{-i\varphi}) \in \operatorname{WF}(\mu), 1 \leq j \leq m \right\}. \end{aligned} \tag{7-5}$$

Definition 7.1 extends the definitions (6-10) for  $m = 0, 1$  and (6-9) for  $m = 2$ . The next theorem extends the WF containments (6-11) for  $\hat{\omega}_1, \hat{\omega}_2$ , to higher  $n$ , locating microlocally the singularities of  $\hat{\omega}_n$ .

**Theorem 7.2.** For any conductivity  $\sigma \in L^\infty(\Omega)$  and all  $n \geq 1$ ,

$$\text{WF}(\hat{\omega}_n) \subset \bigcup \{ \text{Sc}^{(m)}(\mu) : 0 \leq m \leq n, m \equiv n \pmod{2} \}. \quad (7-6)$$

*Proof.* This will follow from (7-1) and the Hörmander–Sato lemma [Hörmander 1971, Theorem 2.5.14]. First, to formulate the  $n$ -fold version of (6-7), we introduce the following notation. For sets  $A, B \subset T^*\mathbb{C}$  and

$$I \in \mathcal{I} := \{ I : I \subset \{1, \dots, n\} \},$$

let

$$\prod_{i \in I} A_i \times \prod_{i' \in I^c} B_{i'} := \{ (z, \zeta) \in T^*\mathbb{C}^{n+1} : (z_i, \zeta_i) \in A \text{ for all } i \in I, (z_{i'}, \zeta_{i'}) \in B, \text{ for all } i' \in I^c \}.$$

For  $I \in \mathcal{I}$ , if we set

$$\text{WF}^I(\mu) := \prod_{i \in I} \text{WF}(\mu)_i \times \prod_{i' \in I^c} 0_{T^*\mathbb{C}, i'}, \quad (7-7)$$

then the analogue of (6-7), which follows from it by induction, is

$$\text{WF}\left(\bigotimes^n \mu\right) \subset \bigcup_{I \in \mathcal{I}, I \neq \emptyset} \text{WF}^I(\mu). \quad (7-8)$$

Next, for  $J \in \mathcal{J}$ , define

$$\bar{J} := \{ i \in \{1, \dots, n\} : i \in J \text{ or } i-1 \in J \} \in \mathcal{I}.$$

Then,  $|\bar{J}|$  is even, and thus

$$|\bar{J}^c| = |\{1, \dots, n\} \setminus \bar{J}| \equiv n \pmod{2}.$$

We can partition  $\bar{J} = \bar{J}_+ \cup \bar{J}_- \cup \bar{J}_\pm$ , where

$$\begin{aligned} \bar{J}_+ &:= \{ i \in \bar{J} : i \in J, i-1 \notin J \}, \\ \bar{J}_- &:= \{ i \in \bar{J} : i-1 \in J, i \notin J \}, \\ \bar{J}_\pm &:= \{ i \in \bar{J} : i-1 \in J, i \in J \}. \end{aligned} \quad (7-9)$$

The submanifold  $L_n^J \subset \mathbb{R} \times \mathbb{S}^1 \times \mathbb{C}^n$  is given by defining functions  $f_0, \{f_j\}_{j \in J}$ , where

$$f_0(t, \varphi, z) = t + (-1)^{n+1} 2 \operatorname{Re} \left( e^{i\varphi} \sum_{i=1}^n (-1)^i z_i \right),$$

$$f_j(t, \varphi, z) = z_j - z_{j+1}, \quad j \in J.$$

The twisted conormal bundles are parametrized by

$$C_n^J = \left\{ \left( t, \varphi, \tau d_{t,\varphi} f_0; z, - \left( \tau d_z f_0 + \sum_{j \in J} \sigma_j \cdot d_z f_j \right) \right) : (t, e^{i\varphi}, z) \in L_n^J, (\tau, \sigma) \in (\mathbb{R} \times \mathbb{C}^{|\bar{J}|}) \setminus \{0\} \right\}.$$

The twisted gradients  $df' := (d_{t,\varphi} f, -d_z f)$  of the defining functions are

$$df'_0 = \left( 1, (-1)^{n+1} 2 \operatorname{Im} \left( e^{i\varphi} \sum_{i=1}^n (-1)^i z_i \right), (-1)^n 2E(\varphi) \right),$$

with  $E(\varphi) = (e^{-i\varphi}, -e^{-i\varphi}, e^{-i\varphi}, \dots, (-1)^n e^{-i\varphi})$ , where we identify  $\pm e^{-i\varphi} \in \mathbb{C}$  with a real covector  $(\xi_i, \eta_i) \in T^*\mathbb{C}$ , and

$$df'_j = -\sigma_j \cdot dz_j + \sigma_j \cdot dz_{j+1}, \quad j \in J,$$

similarly identifying  $\sigma_j \in \mathbb{C}$  with  $(\operatorname{Re} \sigma_j, \operatorname{Im} \sigma_j) \in T^*\mathbb{C}$ . Thus,

$$C_n^J = \left\{ \left( (-1)^n 2 \operatorname{Re} \left( e^{i\varphi} \sum_{i=1}^n (-1)^i z_i \right), e^{i\varphi}, \tau, (-1)^{n+1} 2\tau \operatorname{Im} \left( e^{i\varphi} \sum_{i=1}^n (-1)^i z_i \right); \right. \right. \\ \left. \left. z, (-1)^n 2\tau E(\varphi) + \sum_{i \in \bar{J}_+} \sigma_i \cdot dz_i - \sum_{i \in \bar{J}_-} \sigma_i \cdot dz_i + \sum_{i \in \bar{J}_\pm} (-\sigma_{i-1} + \sigma_i) \cdot dz_i \right) \right. \\ \left. : e^{i\varphi} \in \mathbb{S}^1, z_j - z_{j+1} = 0, j \in J, (\tau, \sigma) \in (\mathbb{R} \times \mathbb{C}^{|J|}) \setminus 0 \right\}. \quad (7-10)$$

Since  $\operatorname{WF}(K_n^{z_0})' = \bigcup_{J \in \mathcal{J}} C_n^J$ , to prove (7-6), it suffices to show that each of the  $2^{n-1}(2^n - 1)$  compositions  $C_n^J \circ \operatorname{WF}^I$ ,  $J \in \mathcal{J}$ ,  $I \in \mathcal{I} \setminus \{\emptyset\}$ , is contained in one of the  $\operatorname{Sc}^{(m)}(\mu)$  for some  $0 \leq m \leq n$  with  $m \equiv n \pmod 2$ . In fact, from (7-7) and the representation of  $C_n^J$  above, one sees that each  $C_n^J \circ \operatorname{WF}^I$  is either empty (e.g., if  $\bar{J}^c \cap I^c \neq \emptyset$ ), or a (potentially) nonempty subset of  $\operatorname{Sc}^{(m)}(\mu)$ , when  $m = |\bar{J}^c| \equiv n \pmod 2$ , yielding (7-6) and finishing the proof of Theorem 7.2.  $\square$

### 8. Parity symmetry

We now come to an important symmetry property which significantly improves the imaging obtained via our reconstruction method. Recall that what we have been denoting by  $\hat{\omega}$  is in fact  $\hat{\omega}^+$ , the partial Fourier transform of the correction term  $\omega^+$  in the CGO solution (3-6) of the Beltrami equation (3-4) with multiplier  $\mu$ . Similarly, the solution  $\omega^-$  in (3-6) corresponding to  $-\mu$  has partial Fourier transform  $\hat{\omega}^-$ . Astala and Päiväranta [2006a] showed that both  $\omega^+$  and  $\omega^-$  can be reconstructed from the Dirichlet-to-Neumann map  $\Lambda_\sigma$ . We show that by taking their difference we can suppress the  $\hat{\omega}_n$  for even  $n$ , and thus suppress some of the singularities described in the preceding sections, most importantly the strong singularity at  $\operatorname{Sc}^{(0)}(\mu) \subset N^*\{t = 0\}$  coming from  $\hat{\omega}_2$ .

Start by writing the two Neumann series

$$\hat{\omega}^+ \sim \sum_{n=1}^{+\infty} \hat{\omega}_n^+ = \hat{\omega}_{\text{odd}}^+ + \hat{\omega}_{\text{even}}^+, \quad \hat{\omega}^- \sim \sum_{n=1}^{+\infty} \hat{\omega}_n^- = \hat{\omega}_{\text{odd}}^- + \hat{\omega}_{\text{even}}^-,$$

where  $\hat{\omega}_{\text{odd}}^\pm$  (resp.  $\hat{\omega}_{\text{even}}^\pm$ ) consists of the  $n$  odd (resp. even) terms in the expansion corresponding to  $\hat{\omega}^\pm$ . Recall that, as a function of  $\mu$ ,  $\hat{\omega}_n^\pm$  is a multilinear form of degree  $n$ .

**Proposition 8.1.** *Each of  $\hat{\omega}_{\text{odd}}^+$  and  $\hat{\omega}_{\text{even}}^+$  has the same parity in  $t$  as the multilinear degrees of its terms; i.e.,*

$$\hat{\omega}_{\text{odd}}^+ = -\hat{\omega}_{\text{odd}}^- \quad \text{and} \quad \hat{\omega}_{\text{even}}^+ = \hat{\omega}_{\text{even}}^-. \quad (8-1)$$

Equivalently,

$$\hat{\omega}_{\text{odd}}^+ = \frac{\hat{\omega}^+ - \hat{\omega}^-}{2} \quad \text{and} \quad \hat{\omega}_{\text{even}}^+ = \frac{\hat{\omega}^+ + \hat{\omega}^-}{2}. \quad (8-2)$$

*Proof.* Let  $\bar{u}^\pm = -\bar{\partial}\omega^\pm$ . As in Section 3,  $u^\pm$  is the solution of the integral equation (3-14),

$$(I + A^\pm \rho)u^\pm = \mp \bar{\alpha}, \tag{8-3}$$

where  $A^\pm = \mp(\bar{\alpha}P + \bar{\nu}S)$ , and  $\alpha$  and  $\nu$  were defined in (3-8). Since  $A^+ = -A^-$  we have  $u_1^+ = -\bar{\alpha} = -u_1^-$ ,  $u_2^+ = -A^+ \bar{u}_1^+ = -(-A^-(-\bar{u}_1^-)) = u_2^-$  and by induction, for  $n \geq 1$ ,

$$u_{n+2}^+ = A^+ \overline{A^+ \bar{u}_n^+} = (-1)^n A^- \overline{A^- \bar{u}_n^-} = (-1)^n u_{n+2}^-.$$

(Another way of seeing this is that  $\mu \rightarrow \hat{\omega}_n$  is a form of degree  $n$ , with the same multilinear kernel applied to both  $\pm\mu$ .) □

Proposition 8.1 provides a method to isolate the even and the odd terms in the expansion of  $\hat{\omega}$ . In particular, by imaging using  $\hat{\omega}_{\text{odd}}^+$ , we can eliminate the strong singularities of  $\hat{\omega}_2$  at  $\text{Sc}^{(0)}(\mu) = N^*\{t=0\}$ , described in (6-13), and in fact the singularities there of all the even terms since, by (7-6), these only arise from  $\hat{\omega}_n$  for even  $n$ .

### 9. Multilinear operator theory

Following the analysis of  $\hat{\omega}_2$ , one can also describe the singularities of  $\hat{\omega}_3$ , but now having to restrict away from  $t=0$ . The singularities of  $\hat{\omega}_3$  are of interest, since, after the symmetrization considerations from the previous section are applied,  $\hat{\omega}_3$  is the first higher-order term encountered after  $\hat{\omega}_1$ . Recall from above that, if  $\mu$  is a piecewise smooth function with jumps ( $m = -1$ ),  $\hat{\omega}_2$  has a singularity at  $\text{Sc}^{(0)}(\mu) = N^*\{t=0\}$  as strong as that of  $\hat{\omega}_1$  at  $\text{Sc}^{(1)}(\mu)$ , and that its presence is due to the singularity of  $K_2^{z_0}$  at the submanifold  $L_2^1 = \{t=0\} \subset L_2^\emptyset \subset \mathbb{R} \times \mathbb{S}^1 \times \mathbb{C}^2$ . Similarly, in order to analyze  $\hat{\omega}_3$ , we will need to localize  $K_3^{z_0}$  away from  $L_3^{12} = \{t=0\} \subset \mathbb{R} \times \mathbb{S}^1 \times \mathbb{C}^3$ , which results in a kernel that can then be decomposed into a sum of two kernels, each having singularities on one of two nested pairs,  $L_3^1 \subset L_3^\emptyset$  or  $L_3^2 \subset L_3^\emptyset$ , but not at  $L_3^1 \cap L_3^2 = L_3^{12} = \{t=0\}$ . We will show that applying these to  $\mu \otimes \mu \otimes \mu$ , as in (7-1), does not just result in terms with WF contained in  $\text{Sc}^{(3)}(\mu) \cup \text{Sc}^{(1)}(\mu)$ , as was shown in Theorem 7.2, but a more precise statement can be made:

**Theorem 9.1.** *If  $\mu \in I^m(\gamma)$  with  $\gamma$  satisfying the curvature condition (6-12), then  $\text{Sc}^{(3)}(\mu)$ , defined as in (6-9), is a smooth Lagrangian manifold in  $T^*(\mathbb{R} \times \mathbb{S}^1) \setminus 0$ , and*

$$\hat{\omega}_3|_{t \neq 0} \in I^{3m+2, -1/2}(\text{Sc}^{(3)}(\mu), \text{Sc}^{(1)}(\mu)). \tag{9-1}$$

**Remark.** For  $m = -1$ , this is in  $I^{-1}(\text{Sc}^{(1)}(\mu) \setminus \text{Sc}^{(3)}(\mu))$ , and thus is half a derivative smoother than  $\hat{\omega}_1$  on  $\text{Sc}^{(1)}(\mu)$ . On the other hand, it is also in  $I^{-3/2}(\text{Sc}^{(3)}(\mu) \setminus \text{Sc}^{(1)}(\mu))$ , which is a full derivative smoother than  $\hat{\omega}_1$ .

To put this in perspective we first discuss what should be the leading terms contributing to  $\hat{\omega}_n$  for general  $n \geq 3$ . The analysis for  $\hat{\omega}_3|_{t \neq 0}$  given below applies more generally to  $\hat{\omega}_n$  if we localize  $K_n^{z_0}$  even more strongly: not just away from  $t=0$ , but away from *all* of the submanifolds  $L_n^J \subset \mathbb{R} \times \mathbb{S}^1 \times \mathbb{C}^n$  with  $|J| \geq 2$ . Now, for  $j \neq j'$ , we have  $L_n^j \cap L_n^{j'} = L_n^{jj'}$ ; by localizing away from all of the  $L_n^J$  with  $|J| = 2$ , by a partition of unity the kernel  $K_n^{z_0}$  can be decomposed into a sum of  $n - 1$  terms, each a nested conormal

distribution associated with the pair  $L_n^\phi \supset L_n^j$ ,  $j = 1, \dots, n - 1$  respectively. When these pieces of  $K_n^{z_0}$  are applied to  $\otimes^n \mu$ , as in (7-1), the results have WF in  $\text{Sc}^{(n)}(\mu) \cup \text{Sc}^{(n-2)}(\mu)$ , and again can be shown to belong to  $I^{p,l}(\text{Sc}^{(n)}(\mu), \text{Sc}^{(n-2)}(\mu))$ . However, as this requires localizing away from  $\bigcup_{|J| \geq 2} L_n^J$ , which is strictly larger than  $L_n^{12 \dots (n-1)}$  if  $n \geq 4$ , the analysis here is inconclusive concerning the singularities of  $\hat{\omega}_n|_{t \neq 0}$ , and thus we only present the details for  $\hat{\omega}_3$ .

We now start the proof of Theorem 9.1 by noting that, for  $n = 3$ , the lattice of submanifolds (7-3) to which the trilinear operator  $T_3^{z_0}$  is associated is a simple diamond,  $L_3^\emptyset \supset L_3^1, L_3^2 \supset L_3^{12}$ . In the region  $\{t \neq 0\}$ , the two submanifolds  $L_3^1$  and  $L_3^2$  are disjoint. Hence, by a partition of unity in the spatial variables, we can write

$$\hat{\omega}_3|_{t \neq 0} = \langle K_3^1 + K_3^2, \mu \otimes \mu \otimes \mu \rangle, \tag{9-2}$$

where each  $K_3^j$  is associated with the nested pair  $L_3^\emptyset \supset L_3^j$ ,  $j = 1, 2$ . Since these two terms are so similar, we just treat the  $K_3^2$  term.

The submanifolds  $L_2^2 \subset L_3^\emptyset \subset \mathbb{R} \times \mathbb{S}^1 \times \mathbb{C}^3$  are given by

$$\begin{aligned} L_3^\emptyset &= \{t - 2 \operatorname{Re}(e^{i\varphi}(z_1 - z_2 + z_3)) = 0\}, \\ L_3^2 &= \{t - 2 \operatorname{Re}(e^{i\varphi}(z_1 - z_2 + z_3)) = 0, z_2 - z_3 = 0\}. \end{aligned} \tag{9-3}$$

For  $K_3^2$  we are localizing away from  $L_3^1$ , so that  $z_1 - z_2 \neq 0$  on the support of the kernels below. Thus, the factors  $(\bar{z}_1 - \bar{z}_2)^{-1+\epsilon_1}$  in (7-2) are smooth, and their dependence on  $\epsilon_1$  is irrelevant for this analysis. Thus,  $K_3^2$  is a sum of two terms, each of which we will still denote  $K_3^2$ , given by

$$K_3^2 = \int_{\mathbb{R}^3} e^{i[\tau(t - 2 \operatorname{Re}(e^{i\varphi}(z_1 - z_2 + z_3))) + (z_2 - z_3) \cdot \sigma]} a_{p,l}(*; \tau; \sigma) d\tau d\sigma, \tag{9-4}$$

where  $*$  denotes the spatial variables and  $a_{p,l}$  is a symbol-valued symbol of biorder  $(3, -1)$  and  $(2, 0)$ , respectively.

If, for any  $c > 0$ , we introduce a smooth cutoff into the amplitude which is a function of  $|\sigma|/|\tau|$  and supported in the region  $\{|\sigma| \geq c|\tau|\}$ , the amplitude becomes a standard symbol of order  $p + l = 2$  in the phase variables  $(\tau, \sigma) \in \mathbb{R}^3 \setminus 0$ . The phase function is nondegenerate and parametrizes the canonical relation, with  $C_0$  as in (5-9),

$$\begin{aligned} C_{0 \times N} &:= C_0 \times N^* \{z_2 = z_3\} \\ &= \{(2 \operatorname{Re}(e^{i\varphi} z_1), e^{i\varphi}, \tau, 2\tau \operatorname{Im}(e^{i\varphi} z_1); z_1, z_2, z_2, 2\tau e^{-i\varphi}, \zeta_2, -\zeta_2) \\ &\quad : e^{i\varphi} \in \mathbb{S}^1, (z_1, z_2) \in \mathbb{C}^2, (\tau, \zeta_2) \in \mathbb{R}^3 \setminus 0\}. \end{aligned}$$

This is a nondegenerate canonical relation: the projection  $\pi_R : C_{0 \times N} \rightarrow T^*\mathbb{C}^3 \setminus 0$  is an immersion and the projection  $\pi_L : C_{0 \times N} \rightarrow T^*(\mathbb{R} \times \mathbb{S}^1) \setminus 0$  is a submersion. Thus, this contribution to  $K_3^2$  belongs to  $I^{2+3/2-8/4}(C_{0 \times N}) = I^{3/2}(C_{0 \times N})$ . Due to the support of the amplitude of this term,  $\pi_R(C_{0 \times N}) \subset \{|\zeta_1| \sim |\zeta_2| = |\zeta_3|\}$ , and by reasoning similar to that used in the analysis of  $\hat{\omega}_1$ , one concludes that

$\mu \otimes \mu \otimes \mu \in I^{3m}(N^*(\gamma \times \gamma \times \gamma))$  microlocally on this region. Hence, the composition

$$C_{0 \times N} \circ N^*(\gamma \times \gamma \times \gamma) \subset C_0 \circ N^*\gamma =: \text{Sc}^{(1)}(\mu)$$

is covered by the transverse intersection calculus, and this contribution to  $\hat{\omega}_3$  belongs to

$$I^{3m+3/2}(\text{Sc}^{(1)}(\mu)). \quad (9-5)$$

Now consider the contribution to (9-4) from the region  $\{|\sigma| \leq \frac{1}{2}|\tau|\}$ . Writing out the representations of each of the three  $\mu$  factors in (9-2) as conormal distributions, we first note that, using the parametrization in (7-10) for  $C_3^2$  and the constraint  $|\sigma| \leq \frac{1}{2}|\tau|$ , we can read off that, on  $\pi_R$  of the wave front relation,

$$|\zeta_1| = 2|\tau| \quad \text{and} \quad |\zeta_j| = |\pm(\sigma - 2\tau e^{-i\varphi})| \geq \frac{3}{2}|\tau|, \quad j = 2, 3.$$

Hence, again we are acting on a part of  $\mu \otimes \mu \otimes \mu$  which is microlocalized where  $|\zeta_1| \sim |\zeta_2| \sim |\zeta_3|$ . As a result, in (9-6) below, the  $\theta_j$  are grouped with  $\tau$  as “elliptic” variables for the symbol-valued symbol estimates. Mimicking the analysis in and following (6-16), homogenize  $z_1, z_2, z_3$  by setting  $\eta_j = \tau z_j$ ,  $j = 1, 2, 3$ . This leads to the expression

$$\int e^{i\tilde{\Psi}} a_{\tilde{p}, \tilde{l}}(*; (\tau, \theta_1, \theta_2, \theta_3, \eta_1, \eta_2, \eta_3); \sigma) d\tau d\theta_1 d\theta_2 d\theta_3 d\eta_1 d\eta_2 d\eta_3 d\sigma, \quad (9-6)$$

with phase

$$\begin{aligned} \tilde{\Psi} &= \tilde{\Psi}(t, e^{i\varphi}; \tau, \theta_1, \theta_2, \theta_3, \eta_1, \eta_2, \eta_3; \sigma) \\ &:= \tau t - 2 \operatorname{Re}(e^{i\varphi}(\eta_1 - \eta_2 + \eta_3)) + \theta_1 g\left(\frac{\eta_1}{\tau}\right) + \theta_2 g\left(\frac{\eta_2}{\tau}\right) + \theta_3 g\left(\frac{\eta_3}{\tau}\right) + \sigma \cdot \left(\frac{\eta_2 - \eta_3}{\tau}\right) \end{aligned}$$

on  $(\mathbb{R} \times \mathbb{S}^1) \times (\mathbb{R}_{\tau, \theta_1, \theta_2, \theta_3, \eta_1, \eta_2, \eta_3}^{10} \setminus \{0\}) \times \mathbb{R}_\sigma^2$  and symbol-valued symbols with biorders  $(\tilde{p}, \tilde{l}) = (3m - 3, -1)$  and  $(3m - 4, 0)$ , respectively. As with the phase  $\tilde{\Phi}$  that arose in the analysis of  $\hat{\omega}_1$ ,  $\tilde{\Psi}$  is a multi-phase function:  $\tilde{\Psi}_0 = \tilde{\Psi}|_{\sigma=0}$  is nondegenerate (excess  $e_0 = 0$ ) and parametrizes  $\text{Sc}^{(3)}(\mu)$ , while the full  $\tilde{\Psi}$  is clean (excess  $e_1 = 1$ ) and parametrizes  $\text{Sc}^{(1)}(\mu)$ . Applying Proposition 6.2, with  $N = 10$ ,  $M = 2$ , the terms in (9-6) with amplitudes of biorders  $(3m - 3, -1)$  and  $(3m - 4, 0)$ , respectively, yield elements of  $I^{3m+2, -1/2}(\text{Sc}^{(3)}(\mu), \text{Sc}^{(1)}(\mu))$  and  $I^{3m+2, -3/2}(\text{Sc}^{(3)}(\mu), \text{Sc}^{(1)}(\mu))$ , respectively; since the former space contains the latter, and furthermore contains the space in (9-5), we conclude that  $\hat{\omega}_3|_{t \neq 0} \in I^{3m+2, -1/2}(\text{Sc}^{(3)}(\mu), \text{Sc}^{(1)}(\mu))$ . This finishes the proof of Theorem 9.1.  $\square$

## 10. Computational studies

In the idealized infinite-bandwidth model discussed above, knowledge of  $\omega_1(z_0, k)$  for all complex frequencies  $k$ , and thus  $T_1^{z_0} \mu = \hat{\omega}(z_0, t, e^{i\varphi})$  for all  $(t, e^{i\varphi})$ , determines  $\mu \bmod C^\infty$ . A more physically realistic model, band-limiting to  $|k| \leq k_{\max}$ , requires a windowed Fourier transform; see [Isaacson et al. 2004; 2006; Knudsen 2003; Knudsen et al. 2004; 2007; Vainikko 2000]. This corresponds to convolving in the  $t$ -variable with a smooth cutoff at length-scale  $\sim k_{\max}^{-1}$ , rendering the reconstruction less accurate. This section examines numerical simulations and how they are affected by this bandwidth issue.

We first introduce a new reconstruction algorithm from the Dirichlet-to-Neumann map  $\Lambda_\sigma$ , as well as the algorithm used in the simulations. Then we will present our numerical results. In this section we take  $\Omega$  to be the unit disk,  $\Omega = D(0, 1)$ .

**10A. Reconstruction algorithm.** The results presented in the preceding sections give rise to a linear reconstruction scheme to approximately recover a conductivity  $\sigma$  from its Dirichlet-to-Neumann map  $\Lambda_\sigma$ . This can be summarized in the following steps:

- (i) Find  $f_{\pm\mu}(z, k)$ , and so  $\omega^\pm(z, k)$ , for  $z \in \partial\Omega$  and  $k \in \mathbb{C}$ , by solving the boundary integral equation

$$f_{\pm\mu}(z, k) + e^{ikz} = (\mathcal{P}_{\pm\mu} + \mathcal{P}_0^k) f_{\pm\mu}(z, k), \quad z \in \partial\Omega, \quad (10-1)$$

where  $\mathcal{P}_{\pm\mu}$  and  $\mathcal{P}_0^k$  are projection operators constructed from  $\Lambda_\sigma$ . See [Astala and Päiväranta 2006a] and [Mueller and Siltanen 2012, Section 16.3.3] for full details.

- (ii) Write  $k = \tau e^{i\varphi}$ . Apply the one-dimensional Fourier transform  $\mathcal{F}_{\tau \mapsto t}$  and the complex average (5-15) in order to obtain  $\hat{\omega}^{a,\pm}(t, e^{i\varphi})$ , with  $a \equiv 1/\sqrt{2}$ .
- (iii) Taking into account the parity result Proposition 8.1, define  $\hat{\omega}_{\text{diff}}^a := \frac{1}{2}(\hat{\omega}^{a,+} - \hat{\omega}^{a,-})$ . Apply either the exact inversion formula (5-18) or the  $\Lambda$ -tomography analogue (5-17) with  $\hat{\omega}_{\text{diff}}^a$  instead of  $\hat{\omega}_1^a$ , in order to obtain an approximation  $\mu_{\text{appr}}$  to  $\mu$ .
- (iv) The approximate conductivity is found with the identity  $\sigma_{\text{appr}} = (1 - \mu_{\text{appr}})/(1 + \mu_{\text{appr}})$ .

**10B. High-precision data assumption.** In the numerical reconstructions presented below, the spectral parameter  $k$  ranges in the disk  $\{|k| < R\}$  with cutoff frequency  $R = 60$ . Such a large radius  $R$  is needed for demonstrating the crucial properties of the new method; with a smaller radius the windowing of the Fourier transform would smooth out important features in the CGO solutions.

Using such a large  $R$  in practice would require very high precision EIT measurements, which cannot be achieved by current technology. However, it is possible to evaluate the needed CGO solutions computationally when  $\sigma$  is known. (Remark: it is possible to compute useful reconstructions from real EIT measurements using the new method combined with sparsity-promoting inversion algorithms, but we do not discuss such approaches further in this paper.) This is done as in [Astala et al. 2014] by solving the Beltrami equation

$$\bar{\partial}_z f_\mu(z, k) = \mu(z) \overline{\partial_z f_\mu(z, k)}, \quad (10-2)$$

which yields very accurate solutions even for large  $|k|$ . From the point of view of the classical  $\bar{\partial}$  reconstruction method [Knudsen et al. 2009; Mueller and Siltanen 2003; 2012; Siltanen et al. 2000] for  $C^2$  conductivities, this is the analogue of solving the Lippmann–Schwinger equation to construct the CGO solutions.

In this section the CGO remainders  $\omega^\pm(z, k)$ , with  $z \in \partial\Omega$  and  $|k| < 60$ , are constructed by solving the Beltrami equation following the approach of Huhtanen and Perämäki [2012] (see also [Astala et al. 2014] and Section 3 for more details). We then follow steps (ii)–(iv) of the algorithm in Section 10A to obtain two-dimensional reconstructions.

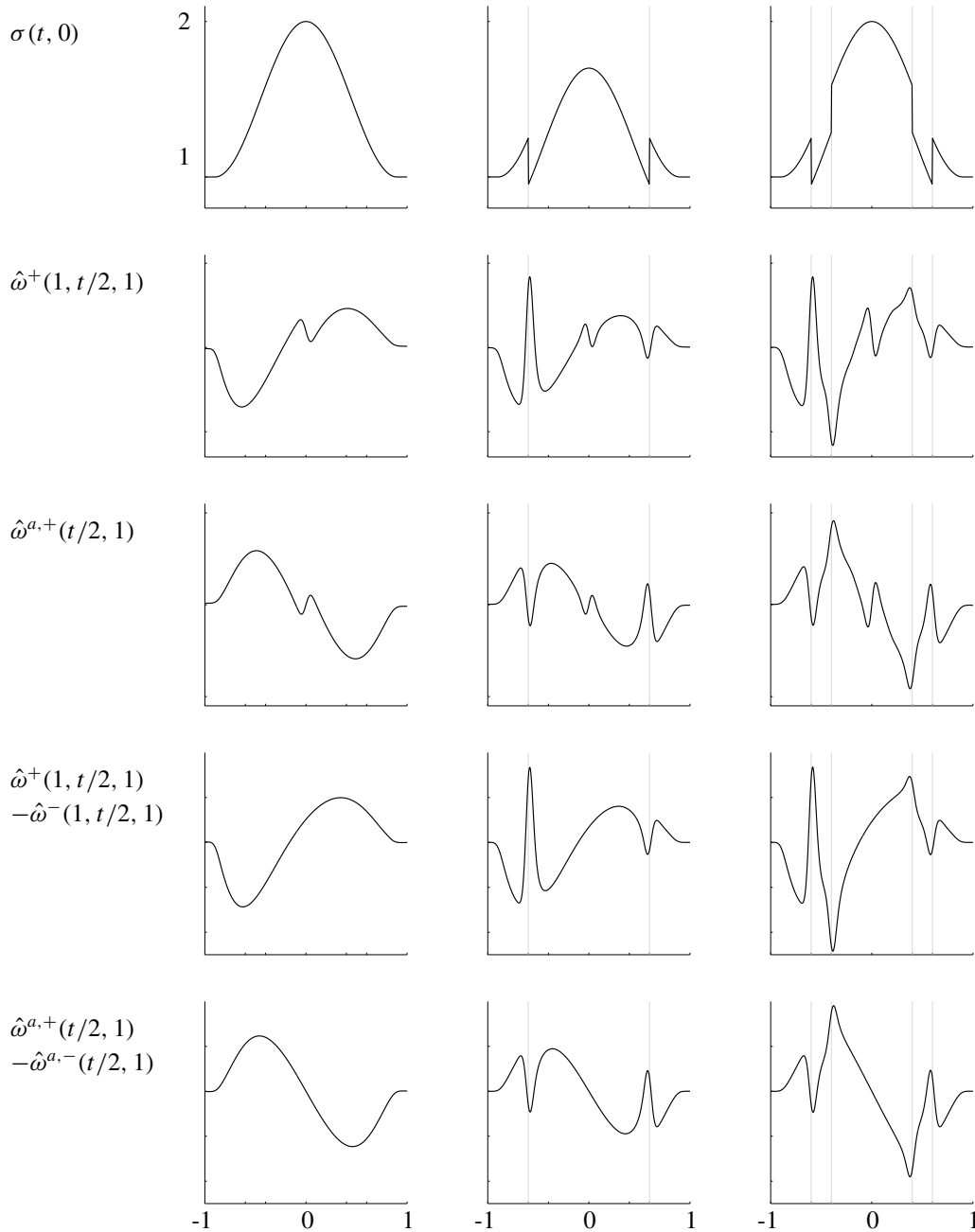


**Figure 6.** Top: profiles of three radial conductivities along the real axis. The middle conductivity has a jump along the circle  $|z| = 0.6$ ; the one on the right has jumps on both  $|z| = 0.4$  and  $|z| = 0.6$ . Rows 2 and 3: the functions  $\hat{\omega}^+(1, t/2, 1)$  and  $\hat{\omega}^{a,+}(t/2, 1)$ , respectively; note the artifacts at  $t = 0$ . Rows 3 and 4: as described in Section 8, the artifacts are eliminated by subtracting  $\hat{\omega}^-$ ,  $\hat{\omega}^{a,-}$ , respectively.

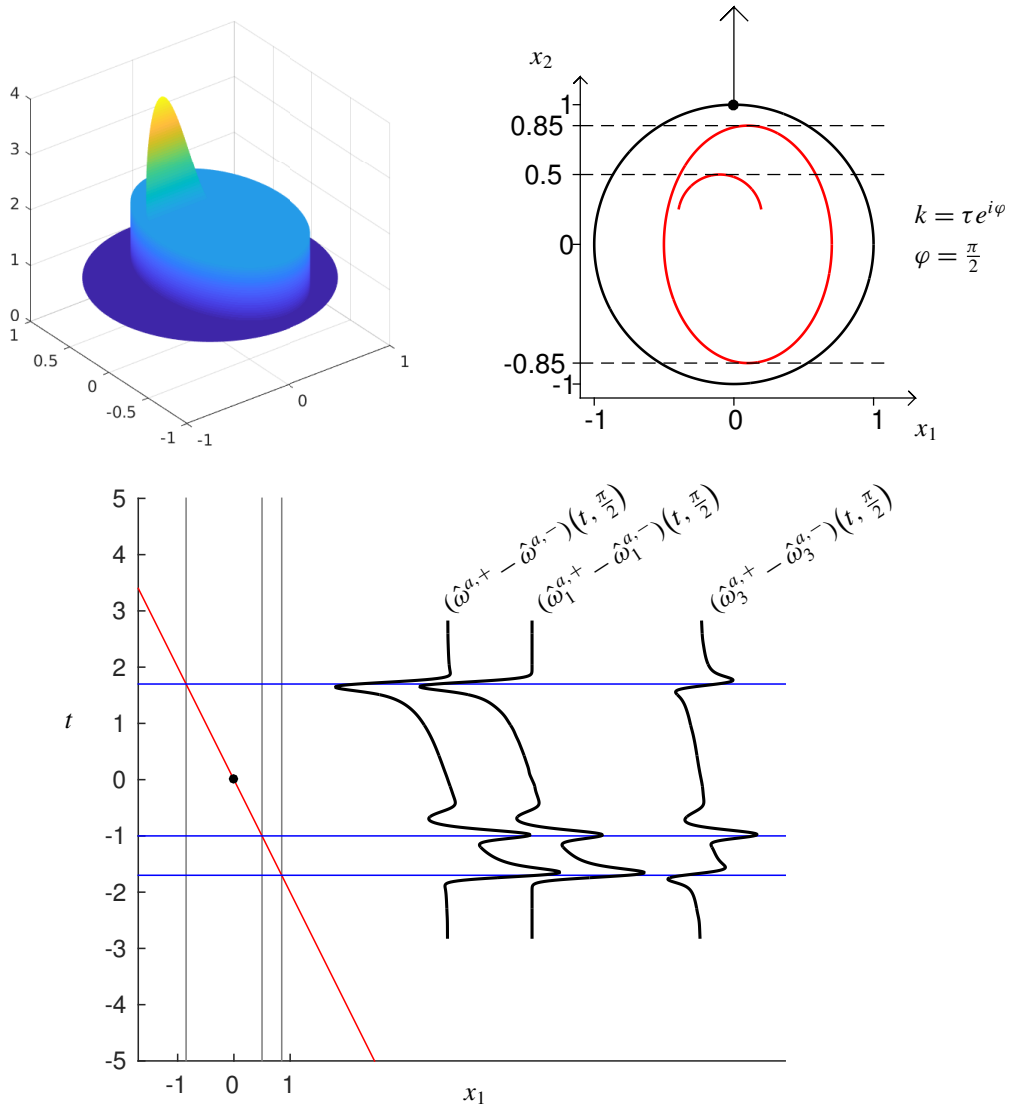


**Figure 7.** Diagram showing the propagation of singularities for the HME phantom with zero background. The virtual direction is  $k = i$ .

**10C. Rotationally symmetric cases.** We study three rotationally symmetric conductivities defined in the unit disc. The first conductivity  $\sigma_1$  is smooth. The second conductivity is defined as

$$\sigma_2 = \sigma_1 - 0.3\chi_{D(0,0.6)}$$

and therefore has a jump of magnitude 0.3 along the circle centered at the origin and radius 0.6. The third rotationally symmetric conductivity is defined as

$$\sigma_3 = \sigma_2 + 0.3\chi_{D(0,0.4)}$$

and has jumps of magnitude 0.3 along the circles centered at the origin and radii 0.4 and 0.6.

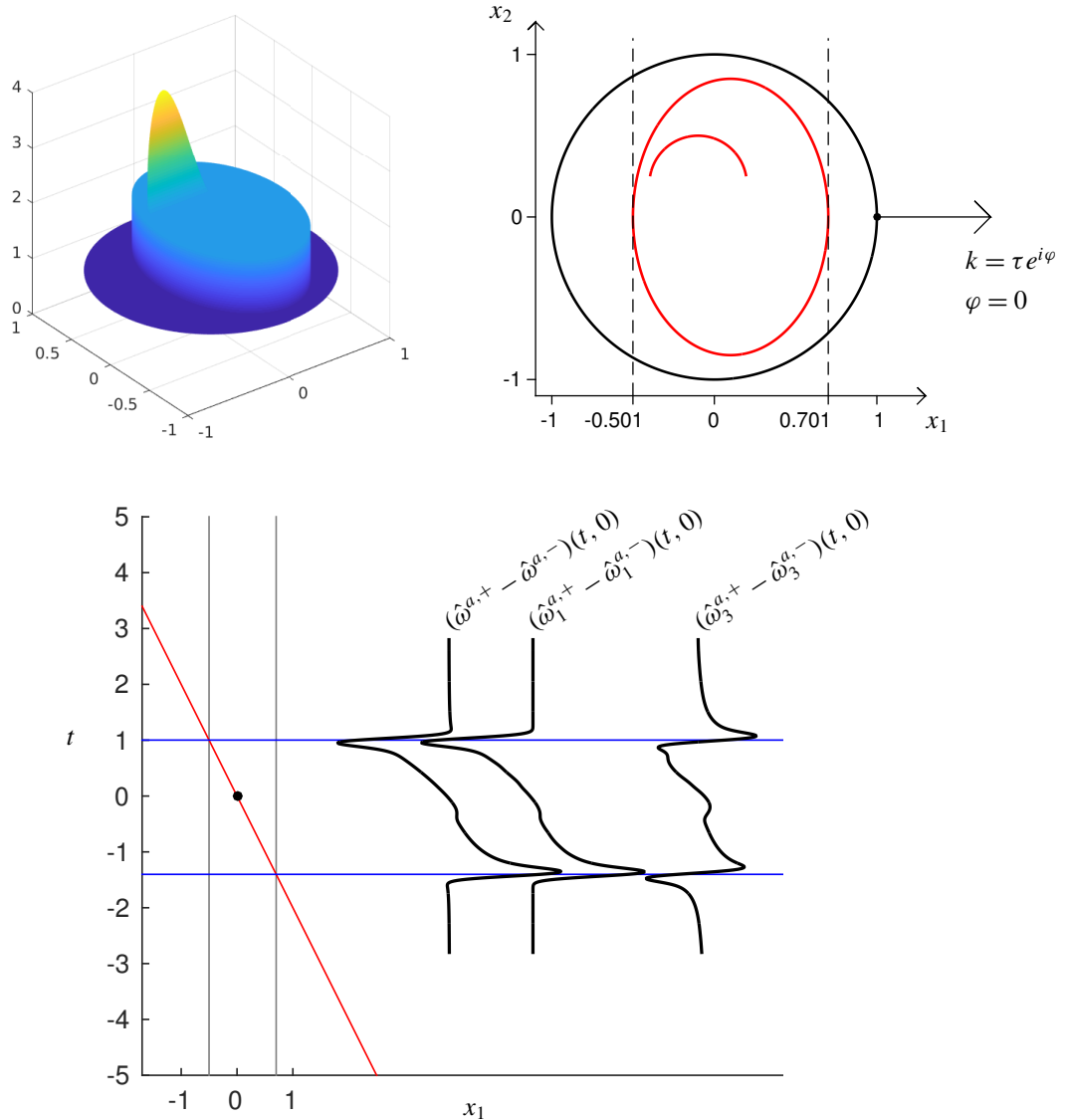


**Figure 8.** Diagram showing the propagation of singularities for the HME phantom with zero background. The virtual direction is  $k = 1$ .

In Figure 6 we show the profiles of  $\hat{\omega}(1, t, 1)$  for three rotationally symmetric conductivity phantoms. The first phantom is smooth, while the second and the third have jumps. The position and the sign of each jump is clearly visible from the CGO-Fourier data. Note that the artifact singularity appearing around 0 in the second and third rows vanishes when considering the difference of the two CGO functions, in the fourth and fifth rows. This confirms the parity symmetry analyzed in Section 8.

**10D. Half-moon and ellipse (HME).** This conductivity phantom has a large elliptical inclusion and another smaller inclusion inside the ellipse. The smaller inclusion has a jump along an almost complete

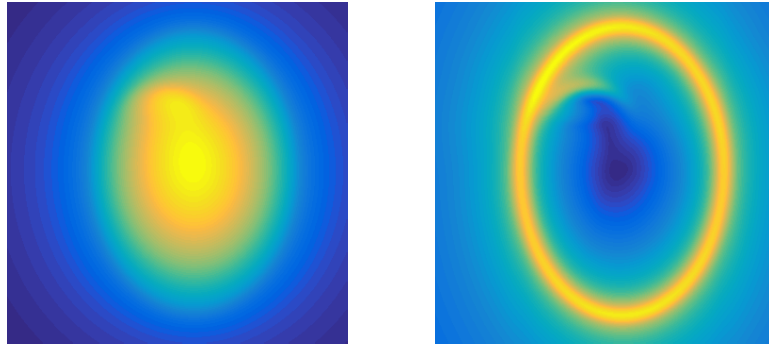


**Figure 9.** Reconstructions from the averaged full series  $\hat{\omega}_{\text{diff}}^a$ . Left: exact inversion formula. Right:  $\Lambda$ -tomography like reconstruction.

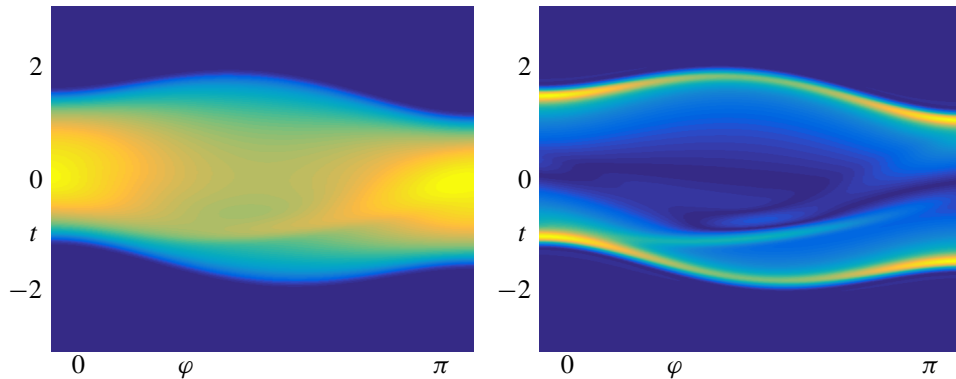


**Figure 10.** Sinograms of the averaged full series  $\hat{\omega}_{\text{diff}}^a$ . Left: exact reconstruction sinogram. Right:  $\Lambda$ -tomography like sinogram.

half-circle. This example was chosen because it has two nontrivial features in the wave front set for the horizontal direction and three for the vertical. Figures 8 and 7 show, in particular, *ladder* diagrams of the propagation of singularities in the directions  $k = i$  and  $k = 1$ , respectively: the zeroth- and second-order terms of the Neumann series for  $\hat{\omega}^a$  are displayed, as well as the full series of the difference of the CGOs:  $\hat{\omega}_{\text{diff}} = (\hat{\omega}^+ - \hat{\omega}^-)/2$ .

Figure 9 shows two-dimensional reconstructions obtained using the new algorithm, with the two different inversion formulas. In Figure 10 we show the values of  $\hat{\omega}_{\text{diff}}^a(t, e^{i\varphi})$  for  $t \in [-3, 3]$  and  $\varphi \in [0, \pi]$ . We borrow the term *sinogram* to describe these plots, because of the clear similarity with the sinograms of X-ray tomography.

## 11. Conclusion

We introduce a novel and robust method for recovering singularities of conductivities from electric boundary measurements. It is unique in its capability of recovering inclusions within inclusions in an unknown inhomogeneous background conductivity. This method provides a new connection between

diffuse tomography (EIT) and classical parallel-beam X-ray tomography and filtered back-projection algorithms.

Full analysis of the higher-order terms  $\hat{\omega}_n$  remains an open problem. We point out that there is a strong formal similarity between the multilinear forms  $\mu \rightarrow \hat{\omega}_n$  and multilinear operators considered by Brown [2001], Nie and Brown [2011] and Perry and Christ [Perry 2016]. Indeed, any Born-type expansion naturally leads to expressions of this general form, with the places of the Cauchy and Beurling kernels for  $\omega_n$  or  $\hat{\omega}_n$  here being taken by the appropriate Green's functions. However, an important feature here is that the singular coefficient in a Beltrami equation occurs in the top-order term, rather than as a potential as in the works cited above. For the application needed in this setting, useful function space estimates do not seem to follow from existing results, which would require higher regularity of  $\mu$ , and this is an interesting topic for future investigation.

## References

- [Alessandrini 1988] G. Alessandrini, "Stable determination of conductivity by boundary measurements", *Appl. Anal.* **27**:1-3 (1988), 153–172. MR Zbl
- [Alessandrini and Di Cristo 2005] G. Alessandrini and M. Di Cristo, "Stable determination of an inclusion by boundary measurements", *SIAM J. Math. Anal.* **37**:1 (2005), 200–217. MR Zbl
- [Alessandrini and Scapin 2017] G. Alessandrini and A. Scapin, "Depth dependent resolution in electrical impedance tomography", *J. Inverse Ill-Posed Probl.* **25**:3 (2017), 391–402. MR Zbl
- [Assenheimer et al. 2001] M. Assenheimer, O. Laver-Moskovitz, D. Malonek, D. Manor, U. Nahaliel, R. Nitzan, and A. Saad, "The T-SCAN technology: electrical impedance as a diagnostic tool for breast cancer detection", *Physiol. Meas.* **22**:1 (2001), 1–8.
- [Astala and Päiväranta 2006a] K. Astala and L. Päiväranta, "A boundary integral equation for Calderón's inverse conductivity problem", *Collect. Math. Spec. Iss.* (2006), 127–139. MR Zbl
- [Astala and Päiväranta 2006b] K. Astala and L. Päiväranta, "Calderón's inverse conductivity problem in the plane", *Ann. of Math. (2)* **163**:1 (2006), 265–299. MR Zbl
- [Astala et al. 2009] K. Astala, T. Iwaniec, and G. Martin, *Elliptic partial differential equations and quasiconformal mappings in the plane*, Princeton Mathematical Series **48**, Princeton Univ. Press, 2009. MR Zbl
- [Astala et al. 2010] K. Astala, J. L. Mueller, L. Päiväranta, and S. Siltanen, "Numerical computation of complex geometrical optics solutions to the conductivity equation", *Appl. Comput. Harmon. Anal.* **29**:1 (2010), 2–17. MR Zbl
- [Astala et al. 2011] K. Astala, J. L. Mueller, L. Päiväranta, A. Perämäki, and S. Siltanen, "Direct electrical impedance tomography for nonsmooth conductivities", *Inverse Probl. Imaging* **5**:3 (2011), 531–549. MR Zbl
- [Astala et al. 2014] K. Astala, L. Päiväranta, J. M. Reyes, and S. Siltanen, "Nonlinear Fourier analysis for discontinuous conductivities: computational results", *J. Comput. Phys.* **276** (2014), 74–91. MR Zbl
- [Astala et al. 2016] K. Astala, M. Lassas, and L. Päiväranta, "The borderlines of invisibility and visibility in Calderón's inverse problem", *Anal. PDE* **9**:1 (2016), 43–98. MR Zbl
- [Brown 2001] R. M. Brown, "Estimates for the scattering map associated with a two-dimensional first-order system", *J. Nonlinear Sci.* **11**:6 (2001), 459–471. MR Zbl
- [Brown and Uhlmann 1997] R. M. Brown and G. A. Uhlmann, "Uniqueness in the inverse conductivity problem for nonsmooth conductivities in two dimensions", *Comm. Partial Differential Equations* **22**:5-6 (1997), 1009–1027. MR Zbl
- [Brühl and Hanke 2000] M. Brühl and M. Hanke, "Numerical implementation of two noniterative methods for locating inclusions by impedance tomography", *Inverse Problems* **16**:4 (2000), 1029–1042. MR Zbl
- [Calderón 1980] A.-P. Calderón, "On an inverse boundary value problem", pp. 65–73 in *Seminar on Numerical Analysis and its Applications to Continuum Physics* (Rio de Janeiro, 1980), Soc. Brasil. Mat., Rio de Janeiro, 1980. MR Zbl

- [Candès and Fernandez-Granda 2013] E. J. Candès and C. Fernandez-Granda, “Super-resolution from noisy data”, *J. Fourier Anal. Appl.* **19**:6 (2013), 1229–1254. MR Zbl
- [Candès and Fernandez-Granda 2014] E. J. Candès and C. Fernandez-Granda, “Towards a mathematical theory of super-resolution”, *Comm. Pure Appl. Math.* **67**:6 (2014), 906–956. MR Zbl
- [Caro and Rogers 2016] P. Caro and K. M. Rogers, “Global uniqueness for the Calderón problem with Lipschitz conductivities”, *Forum Math. Pi* **4** (2016), art. id. e2. MR Zbl
- [Chan and Tai 2004] T. F. Chan and X.-C. Tai, “Level set and total variation regularization for elliptic inverse problems with discontinuous coefficients”, *J. Comput. Phys.* **193**:1 (2004), 40–66. MR Zbl
- [Chen et al. 2001] S. S. Chen, D. L. Donoho, and M. A. Saunders, “Atomic decomposition by basis pursuit”, *SIAM Rev.* **43**:1 (2001), 129–159. MR Zbl
- [Cheney and Isaacson 1992] M. Cheney and D. Isaacson, “Distinguishability in impedance imaging”, *IEEE Trans. Biomed. Eng.* **39**:8 (1992), 852–860.
- [Cheney et al. 1999] M. Cheney, D. Isaacson, and J. C. Newell, “Electrical impedance tomography”, *SIAM Rev.* **41**:1 (1999), 85–101. MR Zbl
- [Chung et al. 2005] E. T. Chung, T. F. Chan, and X.-C. Tai, “Electrical impedance tomography using level set representation and total variational regularization”, *J. Comput. Phys.* **205**:1 (2005), 357–372. MR Zbl
- [Dobson and Santosa 1994] D. C. Dobson and F. Santosa, “An image-enhancement technique for electrical impedance tomography”, *Inverse Problems* **10**:2 (1994), 317–334. MR Zbl
- [van den Doel and Ascher 2006] K. van den Doel and U. M. Ascher, “On level set regularization for highly ill-posed distributed parameter estimation problems”, *J. Comput. Phys.* **216**:2 (2006), 707–723. MR Zbl
- [Duistermaat and Hörmander 1972] J. J. Duistermaat and L. Hörmander, “Fourier integral operators, II”, *Acta Math.* **128**:3–4 (1972), 183–269. MR Zbl
- [Faridani et al. 1992] A. Faridani, E. L. Ritman, and K. T. Smith, “Examples of local tomography”, *SIAM J. Appl. Math.* **52**:4 (1992), 1193–1198. MR Zbl
- [Faridani et al. 1997] A. Faridani, D. V. Finch, E. L. Ritman, and K. T. Smith, “Local tomography, II”, *SIAM J. Appl. Math.* **57**:4 (1997), 1095–1127. MR Zbl
- [Garde and Knudsen 2016] H. Garde and K. Knudsen, “Sparsity prior for electrical impedance tomography with partial data”, *Inverse Probl. Sci. Eng.* **24**:3 (2016), 524–541. MR Zbl
- [Garde and Knudsen 2017] H. Garde and K. Knudsen, “Distinguishability revisited: depth dependent bounds on reconstruction quality in electrical impedance tomography”, *SIAM J. Appl. Math.* **77**:2 (2017), 697–720. MR Zbl
- [Greenleaf and Uhlmann 1990] A. Greenleaf and G. Uhlmann, “Estimates for singular Radon transforms and pseudodifferential operators with singular symbols”, *J. Funct. Anal.* **89**:1 (1990), 202–232. MR Zbl
- [Greenleaf and Uhlmann 2001] A. Greenleaf and G. Uhlmann, “Local uniqueness for the Dirichlet-to-Neumann map via the two-plane transform”, *Duke Math. J.* **108**:3 (2001), 599–617. MR Zbl
- [Greenleaf et al. 2003] A. Greenleaf, M. Lassas, and G. Uhlmann, “The Calderón problem for conormal potentials, I: Global uniqueness and reconstruction”, *Comm. Pure Appl. Math.* **56**:3 (2003), 328–352. MR Zbl
- [Guillemin 1985] V. Guillemin, “On some results of Gelfand in integral geometry”, pp. 149–155 in *Pseudodifferential operators and applications* (Notre Dame, IN, 1984), edited by F. Trèves, Proc. Sympos. Pure Math. **43**, Amer. Math. Soc., Providence, RI, 1985. MR Zbl
- [Guillemin and Sternberg 1977] V. Guillemin and S. Sternberg, *Geometric asymptotics*, Mathematical Surveys **14**, Amer. Math. Soc., Providence, RI, 1977. MR Zbl
- [Guillemin and Uhlmann 1981] V. Guillemin and G. Uhlmann, “Oscillatory integrals with singular symbols”, *Duke Math. J.* **48**:1 (1981), 251–267. MR Zbl
- [Haberman 2015] B. Haberman, “Uniqueness in Calderón’s problem for conductivities with unbounded gradient”, *Comm. Math. Phys.* **340**:2 (2015), 639–659. MR Zbl
- [Haberman and Tataru 2013] B. Haberman and D. Tataru, “Uniqueness in Calderón’s problem with Lipschitz conductivities”, *Duke Math. J.* **162**:3 (2013), 496–516. MR Zbl

- [Hamilton et al. 2012] S. J. Hamilton, C. N. L. Herrera, J. L. Mueller, and A. Von Herrmann, “A direct D-bar reconstruction algorithm for recovering a complex conductivity in 2D”, *Inverse Problems* **28**:9 (2012), art. id. 095005. MR Zbl
- [Hamilton et al. 2014] S. J. Hamilton, A. Hauptmann, and S. Siltanen, “A data-driven edge-preserving D-bar method for electrical impedance tomography”, *Inverse Probl. Imaging* **8**:4 (2014), 1053–1072. MR Zbl
- [Hamilton et al. 2016] S. J. Hamilton, J. M. Reyes, S. Siltanen, and X. Zhang, “A hybrid segmentation and D-bar method for electrical impedance tomography”, *SIAM J. Imaging Sci.* **9**:2 (2016), 770–793. MR Zbl
- [Harrach and Ullrich 2013] B. Harrach and M. Ullrich, “Monotonicity-based shape reconstruction in electrical impedance tomography”, *SIAM J. Math. Anal.* **45**:6 (2013), 3382–3403. MR Zbl
- [Harrach and Ullrich 2015] B. Harrach and M. Ullrich, “Resolution guarantees in electrical impedance tomography”, *IEEE Trans. Med. Imaging* **34**:7 (2015), 1513–1521.
- [Holder 1992a] D. S. Holder, “Detection of cerebral ischaemia in the anaesthetised rat by impedance measurement with scalp electrodes: implications for non-invasive imaging of stroke by electrical impedance tomography”, *Clin. Phys. Physiol. Meas.* **13**:1 (1992), 63–75.
- [Holder 1992b] D. S. Holder, “Electrical impedance tomography with cortical or scalp electrodes during global cerebral ischaemia in the anaesthetised rat”, *Clin. Phys. Physiol. Meas.* **13**:1 (1992), 87–98.
- [Hörmander 1971] L. Hörmander, “Fourier integral operators, I”, *Acta Math.* **127**:1-2 (1971), 79–183. MR Zbl
- [Hörmander 1985] L. Hörmander, *The analysis of linear partial differential operators, IV: Fourier integral operators*, Grundlehren der Mathematischen Wissenschaften **275**, Springer, 1985. MR Zbl
- [Huhtanen and Perämäki 2012] M. Huhtanen and A. Perämäki, “Numerical solution of the  $\mathbb{R}$ -linear Beltrami equation”, *Math. Comp.* **81**:277 (2012), 387–397. MR Zbl
- [Ide et al. 2007] T. Ide, H. Isozaki, S. Nakata, S. Siltanen, and G. Uhlmann, “Probing for electrical inclusions with complex spherical waves”, *Comm. Pure Appl. Math.* **60**:10 (2007), 1415–1442. MR Zbl
- [Ikehata 2000] M. Ikehata, “Reconstruction of the support function for inclusion from boundary measurements”, *J. Inverse Ill-Posed Probl.* **8**:4 (2000), 367–378. MR Zbl
- [Ikehata and Siltanen 2000] M. Ikehata and S. Siltanen, “Numerical method for finding the convex hull of an inclusion in conductivity from boundary measurements”, *Inverse Problems* **16**:4 (2000), 1043–1052. MR Zbl
- [Ikehata and Siltanen 2004] M. Ikehata and S. Siltanen, “Electrical impedance tomography and Mittag–Leffler’s function”, *Inverse Problems* **20**:4 (2004), 1325–1348. MR Zbl
- [Isaacson 1986] D. Isaacson, “Distinguishability of conductivities by electric current computed tomography”, *IEEE Trans. Med. Imaging* **5**:2 (1986), 91–95.
- [Isaacson et al. 2004] D. Isaacson, J. L. Mueller, J. C. Newell, and S. Siltanen, “Reconstructions of chest phantoms by the D-bar method for electrical impedance tomography”, *IEEE Trans. on Med. Imag.* **23** (2004), 821–828.
- [Isaacson et al. 2006] D. Isaacson, J. L. Mueller, J. C. Newell, and S. Siltanen, “Imaging cardiac activity by the D-bar method for electrical impedance tomography”, *Physiol. Meas.* **27**:5 (2006), S43–S50.
- [Jin and Maass 2012] B. Jin and P. Maass, “Sparsity regularization for parameter identification problems”, *Inverse Problems* **28**:12 (2012), art. id. 123001. MR Zbl
- [Kaipio et al. 2000] J. P. Kaipio, V. Kolehmainen, E. Somersalo, and M. Vauhkonen, “Statistical inversion and Monte Carlo sampling methods in electrical impedance tomography”, *Inverse Problems* **16**:5 (2000), 1487–1522. MR Zbl
- [Kim 2008] S. E. Kim, “Calderón’s problem for Lipschitz piecewise smooth conductivities”, *Inverse Problems* **24**:5 (2008), art. id. 055016. MR Zbl
- [Kirsch 1998] A. Kirsch, “Characterization of the shape of a scattering obstacle using the spectral data of the far field operator”, *Inverse Problems* **14**:6 (1998), 1489–1512. MR Zbl
- [Knudsen 2003] K. Knudsen, “A new direct method for reconstructing isotropic conductivities in the plane”, *Physiol. Meas.* **24**:2 (2003), 391–403.
- [Knudsen et al. 2004] K. Knudsen, J. Mueller, and S. Siltanen, “Numerical solution method for the dbar-equation in the plane”, *J. Comput. Phys.* **198**:2 (2004), 500–517. MR Zbl
- [Knudsen et al. 2007] K. Knudsen, M. Lassas, J. L. Mueller, and S. Siltanen, “D-bar method for electrical impedance tomography with discontinuous conductivities”, *SIAM J. Appl. Math.* **67**:3 (2007), 893–913. MR Zbl

- [Knudsen et al. 2009] K. Knudsen, M. Lassas, J. L. Mueller, and S. Siltanen, “Regularized D-bar method for the inverse conductivity problem”, *Inverse Probl. Imaging* **3**:4 (2009), 599–624. MR Zbl
- [Kohn and Vogelius 1985] R. V. Kohn and M. Vogelius, “Determining conductivity by boundary measurements, II: Interior results”, *Comm. Pure Appl. Math.* **38**:5 (1985), 643–667. MR Zbl
- [Kuchment 2014] P. Kuchment, *The Radon transform and medical imaging*, CBMS-NSF Regional Conference Series in Applied Mathematics **85**, Society for Industrial and Applied Mathematics, Philadelphia, PA, 2014. MR Zbl
- [Lechleiter 2006] A. Lechleiter, “A regularization technique for the factorization method”, *Inverse Problems* **22**:5 (2006), 1605–1625. MR Zbl
- [Lechleiter et al. 2008] A. Lechleiter, N. Hyvönen, and H. Hakula, “The factorization method applied to the complete electrode model of impedance tomography”, *SIAM J. Appl. Math.* **68**:4 (2008), 1097–1121. MR Zbl
- [Malone et al. 2014] E. Malone, M. Jehl, S. Arridge, T. Betcke, and D. Holder, “Stroke type differentiation using spectrally constrained multifrequency EIT: evaluation of feasibility in a realistic head model”, *Physiol. Meas.* **35**:6 (2014), 1051–1066.
- [Mandache 2001] N. Mandache, “Exponential instability in an inverse problem for the Schrödinger equation”, *Inverse Problems* **17**:5 (2001), 1435–1444. MR Zbl
- [Melrose and Uhlmann 1979] R. B. Melrose and G. A. Uhlmann, “Lagrangian intersection and the Cauchy problem”, *Comm. Pure Appl. Math.* **32**:4 (1979), 483–519. MR Zbl
- [Mendoza 1982] G. Mendoza, “Symbol calculus associated with intersecting Lagrangians”, *Comm. Partial Differential Equations* **7**:9 (1982), 1035–1116. MR Zbl
- [Mueller and Siltanen 2003] J. L. Mueller and S. Siltanen, “Direct reconstructions of conductivities from boundary measurements”, *SIAM J. Sci. Comput.* **24**:4 (2003), 1232–1266. MR Zbl
- [Mueller and Siltanen 2012] J. L. Mueller and S. Siltanen, *Linear and nonlinear inverse problems with practical applications*, Computational Science & Engineering **10**, Society for Industrial and Applied Mathematics, Philadelphia, PA, 2012. MR Zbl
- [Nachman 1996] A. I. Nachman, “Global uniqueness for a two-dimensional inverse boundary value problem”, *Ann. of Math. (2)* **143**:1 (1996), 71–96. MR Zbl
- [Nagayasu et al. 2009] S. Nagayasu, G. Uhlmann, and J.-N. Wang, “A depth-dependent stability estimate in electrical impedance tomography”, *Inverse Problems* **25**:7 (2009), art. id. 075001. MR Zbl
- [Nie and Brown 2011] Z. Nie and R. M. Brown, “Estimates for a family of multi-linear forms”, *J. Math. Anal. Appl.* **377**:1 (2011), 79–87. MR Zbl
- [Perry 2016] P. A. Perry, “Global well-posedness and long-time asymptotics for the defocussing Davey–Stewartson II equation in  $H^{1,1}(\mathbb{C})$ ”, *J. Spectr. Theory* **6**:3 (2016), 429–481. MR Zbl
- [Phong and Stein 1986] D. H. Phong and E. M. Stein, “Hilbert integrals, singular integrals, and Radon transforms, I”, *Acta Math.* **157**:1-2 (1986), 99–157. MR Zbl
- [Rondi and Santosa 2001] L. Rondi and F. Santosa, “Enhanced electrical impedance tomography via the Mumford–Shah functional”, *ESAIM Control Optim. Calc. Var.* **6** (2001), 517–538. MR Zbl
- [Siltanen et al. 2000] S. Siltanen, J. Mueller, and D. Isaacson, “An implementation of the reconstruction algorithm of A. Nachman for the 2D inverse conductivity problem”, *Inverse Problems* **16**:3 (2000), 681–699. MR Zbl
- [Sylvester and Uhlmann 1987] J. Sylvester and G. Uhlmann, “A global uniqueness theorem for an inverse boundary value problem”, *Ann. of Math. (2)* **125**:1 (1987), 153–169. MR Zbl
- [Tanushev and Vese 2007] N. M. Tanushev and L. A. Vese, “A piecewise-constant binary model for electrical impedance tomography”, *Inverse Probl. Imaging* **1**:2 (2007), 423–435. MR Zbl
- [Uhlmann and Wang 2008] G. Uhlmann and J.-N. Wang, “Reconstructing discontinuities using complex geometrical optics solutions”, *SIAM J. Appl. Math.* **68**:4 (2008), 1026–1044. MR Zbl
- [Vainikko 2000] G. Vainikko, “Fast solvers of the Lippmann–Schwinger equation”, pp. 423–440 in *Direct and inverse problems of mathematical physics* (Newark, DE, 1997), edited by R. P. Gilbert et al., Int. Soc. Anal. Appl. Comput. **5**, Kluwer, Dordrecht, 2000. MR Zbl
- [Zhou et al. 2015] Z. Zhou, G. S. dos Santos, T. Dowrick, J. Avery, Z. Sun, H. Xu, and D. S. Holder, “Comparison of total variation algorithms for electrical impedance tomography”, *Physiol. Meas.* **36**:6 (2015), 1193–1209.

Received 12 Dec 2016. Revised 21 Sep 2017. Accepted 14 Nov 2017.

ALLAN GREENLEAF: [allan.greenleaf@rochester.edu](mailto:allan.greenleaf@rochester.edu)  
*Department of Mathematics, University of Rochester, Rochester, NY, United States*

MATTI LASSAS: [matti.lassas@helsinki.fi](mailto:matti.lassas@helsinki.fi)  
*Department of Mathematics and Statistics, University of Helsinki, Helsinki, Finland*

MATTEO SANTACESARIA: [matteo.santacesaria@helsinki.fi](mailto:matteo.santacesaria@helsinki.fi)  
*Dipartimento di Matematica, Politecnico di Milano, Milano, Italy*

SAMULI SILTANEN: [samuli.siltanen@helsinki.fi](mailto:samuli.siltanen@helsinki.fi)  
*Department of Mathematics and Statistics, University of Helsinki, Helsinki, Finland*

GUNTHER UHLMANN: [guntheruhlmann@gmail.com](mailto:guntheruhlmann@gmail.com)  
*Department of Mathematics, University of Washington, Seattle, WA, United States*



# Analysis & PDE

msp.org/apde

## EDITORS

EDITOR-IN-CHIEF

Patrick Gérard

patrick.gerard@math.u-psud.fr

Université Paris Sud XI

Orsay, France

## BOARD OF EDITORS

Massimiliano Berti	Scuola Intern. Sup. di Studi Avanzati, Italy berti@sissa.it	Clément Mouhot	Cambridge University, UK c.mouhot@dpmms.cam.ac.uk
Sun-Yung Alice Chang	Princeton University, USA chang@math.princeton.edu	Werner Müller	Universität Bonn, Germany mueller@math.uni-bonn.de
Michael Christ	University of California, Berkeley, USA mchrist@math.berkeley.edu	Gilles Pisier	Texas A&M University, and Paris 6 pisier@math.tamu.edu
Alessio Figalli	ETH Zurich, Switzerland alessio.figalli@math.ethz.ch	Tristan Rivière	ETH, Switzerland riviere@math.ethz.ch
Charles Fefferman	Princeton University, USA cf@math.princeton.edu	Igor Rodnianski	Princeton University, USA irod@math.princeton.edu
Ursula Hamenstaedt	Universität Bonn, Germany ursula@math.uni-bonn.de	Sylvia Serfaty	New York University, USA serfaty@cims.nyu.edu
Vaughan Jones	U.C. Berkeley & Vanderbilt University vaughan.f.jones@vanderbilt.edu	Yum-Tong Siu	Harvard University, USA siu@math.harvard.edu
Vadim Kaloshin	University of Maryland, USA vadim.kaloshin@gmail.com	Terence Tao	University of California, Los Angeles, USA tao@math.ucla.edu
Herbert Koch	Universität Bonn, Germany koch@math.uni-bonn.de	Michael E. Taylor	Univ. of North Carolina, Chapel Hill, USA met@math.unc.edu
Izabella Laba	University of British Columbia, Canada ilaba@math.ubc.ca	Gunther Uhlmann	University of Washington, USA gunther@math.washington.edu
Gilles Lebeau	Université de Nice Sophia Antipolis, France lebeau@unice.fr	András Vasy	Stanford University, USA andras@math.stanford.edu
Richard B. Melrose	Massachusetts Inst. of Tech., USA rbm@math.mit.edu	Dan Virgil Voiculescu	University of California, Berkeley, USA dvv@math.berkeley.edu
Frank Merle	Université de Cergy-Pontoise, France Frank.Merle@u-cergy.fr	Steven Zelditch	Northwestern University, USA zelditch@math.northwestern.edu
William Minicozzi II	Johns Hopkins University, USA minicozz@math.jhu.edu	Maciej Zworski	University of California, Berkeley, USA zworski@math.berkeley.edu

## PRODUCTION

production@msp.org

Silvio Levy, Scientific Editor

---

See inside back cover or [msp.org/apde](http://msp.org/apde) for submission instructions.

---

The subscription price for 2018 is US \$275/year for the electronic version, and \$480/year (+\$55, if shipping outside the US) for print and electronic. Subscriptions, requests for back issues from the last three years and changes of subscriber address should be sent to MSP.

---

Analysis & PDE (ISSN 1948-206X electronic, 2157-5045 printed) at Mathematical Sciences Publishers, 798 Evans Hall #3840, c/o University of California, Berkeley, CA 94720-3840, is published continuously online. Periodical rate postage paid at Berkeley, CA 94704, and additional mailing offices.

---

APDE peer review and production are managed by EditFlow<sup>®</sup> from MSP.

PUBLISHED BY

 **mathematical sciences publishers**  
nonprofit scientific publishing

<http://msp.org/>

© 2018 Mathematical Sciences Publishers

# ANALYSIS & PDE

Volume 11 No. 8 2018

---

Invariant measure and long time behavior of regular solutions of the Benjamin–Ono equation	1841
MOUHAMADOU SY	
Rigidity of minimizers in nonlocal phase transitions	1881
OVIDIU SAVIN	
Propagation and recovery of singularities in the inverse conductivity problem	1901
ALLAN GREENLEAF, MATTI LASSAS, MATTEO SANTACESARIA, SAMULI SILTANEN and GUNTHER UHLMANN	
Quantitative stochastic homogenization and regularity theory of parabolic equations	1945
SCOTT ARMSTRONG, ALEXANDRE BORDAS and JEAN-CHRISTOPHE MOURRAT	
Hopf potentials for the Schrödinger operator	2015
LUIGI ORSINA and AUGUSTO C. PONCE	
Monotonicity of nonpluripolar products and complex Monge–Ampère equations with pre- scribed singularity	2049
TAMÁS DARVAS, ELEONORA DI NEZZA and CHINH H. LU	
On weak weighted estimates of the martingale transform and a dyadic shift	2089
FEDOR NAZAROV, ALEXANDER REZNIKOV, VASILY VASYUNIN and ALEXANDER VOLBERG	
Two-microlocal regularity of quasimodes on the torus	2111
FABRICIO MACIÀ and GABRIEL RIVIÈRE	
Spectral distribution of the free Jacobi process, revisited	2137
TAREK HAMDI	



2157-5045(2018)11:8;1-M